Iranian Journal of Numerical Analysis and Optimization
Vol. 15, No. 2, 2025, pp 770–822
https://doi.org/10.22067/ijnao.2025.92092.1596
https://ijnao.um.ac.ir/

Research Article

A numerical algorithm based on Jacobi polynomials for FIDEs with error estimation

K. Sadri*, D. Amilo and E. Hincal

Abstract

This study aims to address a specific class of mathematical problems known as fractional integro-differential equations. These equations are used to model various phenomena,, including heat conduction in materials with

*Corresponding author

Received 8 February 2025; revised 5 March 2025; accepted 14 March 2025

Khadijeh Sadri
Mathematics Research Center, Near East University TRNC, Mersin 10, Nicosia 99138, Turkey., Faculty of Art and Science, University of Kyrenia, Kyrenia, TRNC, Mersin 10, Turkey. e-mail: khadijeh.sadrikhatouni@neu.edu.tr

David Amilo
Mathematics Research Center, Near East University TRNC, Mersin 10, Nicosia 99138, Turkey., Faculty of Art and Science, University of Kyrenia, Kyrenia, TRNC, Mersin 10, Turkey. e-mail: amilodavid.ikechukwu@neu.edu.tr

Evren Hincal
Mathematics Research Center, Near East University TRNC, Mersin 10, Nicosia 99138, Turkey., Faculty of Art and Science, University of Kyrenia, Kyrenia, TRNC, Mersin 10, Turkey., Research Center of Applied Mathematics, Khazar University, Baku, Azerbaijan
e-mail: evren.hincal@neu.edu.tr

How to cite this article
Sadri, K., Amilo, D. and Hincal, E., A numerical algorithm based on Jacobi polynomials for FIDEs with error estimation. *Iran. J. Numer. Anal. Optim.*, 2025; 15(2): 770-822. https://doi.org/10.22067/ijnao.2025.92092.1596

memory, damping laws, diffusion processes, earthquake models, fluid dynamics, traffic flow, and continuum mechanics. This research focuses on problems where the fractional derivative operator is defined in the Caputo sense. Our proposed methodology employs an operational approach based on the use of shifted Jacobi polynomials. We derive operational matrices for fractional integration and product, which are then applied to approximate solutions for both linear and nonlinear problems. By using these matrices in conjunction with the collocation method, we transform the original problem into a system of algebraic equations. Notably, our approach is simpler and more cost-effective compared to established methods such as Adomian decomposition, Homotopy perturbation, Sinc-collocation, and Legendre wavelet techniques. We provide several illustrative examples to validate our method's effectiveness and reliability. Additionally, we present theorems concerning the existence of a unique solution and the convergence of our proposed approach.

AMS subject classifications (2020): Primary 33C45; Secondary 65D15, 34K37, 45J05.

Keywords: Fractional integro-differential equation; Caputo derivative operator; Jacobi polynomials; Operational matrices; Convergence.

1 Introduction

Fractional calculus has gained significant attention from mathematicians and engineers in recent decades due to the widespread use of fractional integral and derivative operators in various disciplines and engineering applications [22, 18, 19, 27, 4]. These operators are relevant in modeling numerous physical phenomena, including heat conduction in materials with memory, damping laws, diffusion processes, earthquake models, fluid dynamics, traffic flow, continuum mechanics, chemistry, acoustics, and psychology [22, 18, 19, 27, 4]. Functional equations of fractional order, such as fractional integro-differential equations (FIDEs), are crucial for accurately modeling these phenomena. The derivatives in these equations typically appear in the Riemann–Liouville and Caputo senses. The Caputo derivative is especially favored in practice due to its physically interpretable initial conditions, which resemble those of integer-order differential equations. In contrast, initial conditions derived from the Riemann–Liouville derivative lack a clear physical interpretation [22, 18, 19, 27, 4]. FIDEs arise in various scientific and engineering fields, such as viscosity measurement in oil exploration, continuum and statistical mechanics, chemical kinetics, fluid dynamics, and biological models [12, 11, 23, 26]. Understanding the properties and physical nature of these equations is crucial, leading many researchers and mathematicians to develop or refine methods for solving integro-differential equations with fractional derivatives. However, solving these equations presents both analytical and numerical challenges, driving the search for effective methods. In this context, Huang et al. [22] extended the Taylor method to solve a generalization of fractional differential, Fredholm integral, and Volterra integral equations. Authors in [16, 15] developed the Homotopy perturbation method to solve both linear and nonlinear FIDEs. The Homotopy analysis method has been applied to solve linear FIDEs in [1], while in [24], the Chebyshev pseudo-spectral method was used to solve systems of FIDEs of the Volterra type. In [25], the authors presented three numerical schemes for solving linear FIDEs. Mokhtary [29] applied a discrete Galerkin method to solve linear FIDEs. Laguerre polynomials and a collocation method were developed in [49] to solve fractional linear Volterra integro-differential equations. Nazari, Shahmorad, and Jahanshahi [31] proposed a quadrature method for solving nonlinear FIDEs of the Hammerstein type. Babaei, Jafari, and Banihashemi [5] introduced a collocation approach based on sixth-kind Chebyshev polynomials to reduce variable-order FIDEs to a system of algebraic equations and determined an approximate solution. Darweesh, Al-Khaled, and Al-Yaqeen [9] used the Laplace Haar wavelet method to solve systems of linear fractional Fredholm integro-differential equations and evaluated the rate of convergence.

Among the many numerical methods developed, spectral methods are particularly notable for their high accuracy and ease of implementation. These methods, including Galerkin, collocation, and tau methods, involve expressing the solution to a functional equation as a linear combination of basis functions, which transforms the original equation into a discrete algebraic form. In this context, Rahimkhani, Ordokhani, and Babolian [34] employed a Bernoulli wavelet operational approach to solve fractional delay differential equations. In [35], the authors introduced generalized fractional-order Bernoulli wavelet functions to obtain numerical solutions for fractional-order pantograph differential equations. In [37], a new technique based on Muntz–Legendre functions and their operational matrices was proposed to solve fractional-order pantograph equations. Bernoulli wavelet functions were also applied to solve delay fractional-order optimal control problems in [33]. Rahimkhani, Ordokhani, and Babolian [36] utilized fractional-order Bernoulli functions to achieve numerical solutions for fractional Fredholm–Volterra integro-differential equations. Rahimkhani and Ordokhani [32] used a Bernoulli wavelet collocation method to solve fractional-order partial differential equations. The Bernstein collocation method was developed in [41] to solve Sylvester matrix differential equations. A method combining Bell polynomials and the Galerkin approach was proposed to address fractional optimal control problems [43]. Sadek and Bataineh [40] presented generalized Bernstein functions and the collocation method to approximate solutions for χ-fractional differential equations. Jacobi orthogonal polynomials are widely used as basis functions in spectral methods. For example, shifted Jacobi polynomials have been employed alongside spectral tau and collocation methods to solve linear and nonlinear multi-term fractional differential equations [13]. Similarly, the shifted Chebyshev spectral tau method has been used to construct numerical solutions for linear multi-order fractional differential equations [6]. A new numerical approach for solving fractional-order pantograph partial differential equations was introduced in [52] by utilizing two-variable Gegenbauer polynomials. The Lucas wavelets, combined with the Legendre–Gauss quadrature rule and modified operational matrices for integration and pseudo-operational fractional derivatives, were used to study the solution of fractional Fredholm–Volterra integro-differential equations [10]. Hosseininia, Heydari, and Avazzadeh [21] proposed the use of orthonormal shifted discrete Legendre polynomials and the collocation method for solving the variable-order fractional extended Fisher–Kolmogorov equation. A finite class of Romanovski–Jacobi polynomials was used as basis functions in the spectral tau method to approximate solutions to time-fractional partial differential equations on a semi-infinite interval [3]. Shifted Jacobi polynomials were employed by Heydari, Zhagharian, and Razzaghi [20] to find numerical solutions to one- and two-dimensional stochastic multi-order fractional diffusion-wave equations. In [2], shifted Jacobi polynomials and a fractional-order shifted Jacobi–Gauss collocation method were applied to solve FIDEs with weakly singular kernels. In [51], shifted sixth-kind Chebyshev polynomials, combined with the collocation method, were used to convert systems of FIDEs with weakly singular kernels into algebraic systems, allowing for approximate solutions. Authors in [7] employed shifted Jacobi polynomials with an operational collocation method to obtain approximate solutions to a class of weakly singular FIDEs. Ebrahimi and Sadri [14] solved fractional-order pantograph differential equations by introducing fractional-order Jacobi functions based on Jacobi polynomials, presenting a relationship between the basis functions with delay and the original Jacobi polynomials. These examples highlight the versatility and effectiveness of spectral methods in solving FIDEs and related problems.

In this paper, we extend the use of classical orthogonal Jacobi polynomials to solve both linear and nonlinear integro-differential equations with fractional orders of arbitrary nature. Specifically, we focus on three distinct types of these equations:

$$D^{\nu}y(t)+h(t)\,y(t)+\int_0^t k(t,s)\,y(s)\,ds+\int_0^t \tilde{k}(t,s)\,D^{\gamma}y(s)\,ds=f(t),\quad 0\leqslant t\leqslant 1,\quad 0<\gamma<\nu\leqslant m,$$

$$y''(t)+h(t)\,y'(t)+g(t)\,D^{\nu}y(t)+\int_0^t k(t,s)\,y(s)\,ds=f(t),\qquad 0\leqslant t\leqslant 1,\quad 0<\nu<2,$$

$$D^{\nu}y(t)+h(t)\,y(t)+\lambda_1\int_0^t k(t,s)\,y^2(s)\,ds+\lambda_2\int_0^1 \tilde{k}(t,s)\,y^2(s)\,ds=f(t),\quad 0\leqslant t\leqslant 1.$$

Under appropriate initial conditions, let $\nu,\gamma\in\mathbb{R}$, $m\in\mathbb{Z}^+$, and f,g,h,k, and $\tilde{k}$ be known and continuous real-valued functions. The function y is unknown, and λ_1 and λ_2 are real numbers. As the first step in our solution approach, we derive the fractional operational matrices for integration and multiplication through straightforward algebraic computations, thus reducing computational costs. These resulting matrices and approximations are then substituted into the original problem, transforming it into a corresponding system of algebraic equations. This system is subsequently collocated at the $N+1$ roots of the $N+1$th shifted Jacobi polynomials, $P_{N+1}^{(\alpha,\beta)}(t)$, where

$t \in [0, 1]$. Notably, Jacobi polynomials are parameterized by α and β, both of which are greater than -1. By varying these parameters, different variants of this family of orthogonal polynomials can be obtained. Solving the resulting system gives an approximate solution, denoted as $y_N(t)$. For handling nonlinear systems, we employ the well-known Newton's iteration method. Additionally, we provide a convergence analysis of our proposed method within a Jacobi-weighted Sobolev space.

The contributions of this paper can be summarized as follows:

- Enhanced precision compared to existing methods.
- Flexibility in adjusting parameters α and β, enabling investigation into their impact on obtained solutions.
- Computation of error bounds for resulting approximate solutions within a Jacobi-weighted Sobolev space.
- Estimation of errors in approximate solutions in scenarios where exact solutions are unknown, allowing comparison with absolute errors.

The novelty of this research lies in its innovative application of the Jacobi operational method to solve a wide range of integro-differential equations (IDEs) featuring fractional derivatives of arbitrary order ν. By harnessing the versatility of shifted Jacobi polynomials on the interval $[0, 1]$, the study introduces a novel approach to transforming complex IDEs—both linear and nonlinear—into more manageable algebraic equations. This method not only simplifies the solution process but also offers a systematic framework for determining coefficients and constructing operational matrices for fractional integration and product. Furthermore, the study delves into investigating the existence, uniqueness, and convergence of solutions, shedding light on the method's theoretical underpinnings and practical efficacy. Through illustrative examples and comparative analyses with existing methods, the research showcases the superior accuracy and computational efficiency of the proposed approach, positioning it as a promising tool for tackling a broad spectrum of functional equations. The organization of this paper is as follows:

- Section 1 introduces the topic.

- Section 2 provides preliminary definitions and concepts of fractional calculus.
- Section 3 delves into the existence and uniqueness of solutions for the equations under consideration.
- Section 4 discusses shifted Jacobi polynomials and their properties, along with deriving their operational matrices of fractional integration and product.
- Section 5 presents and proves theorems regarding the convergence of the proposed method.
- Section 6 offers several examples to illustrate the simplicity and efficiency of our proposed method.
- Finally, section 7 contains discussions and conclusions.

2 Preliminaries

Despite the various definitions of fractional-order derivative and integral operators, such as the Θ-conformable fractional derivatives [39], Caputo cotangent fractional derivatives [38], Hilfer cotangent fractional derivatives [42], and q-trigonometric derivatives [44], the Caputo derivative and Riemann–Liouville integral operators remain popular and widely used. Some definitions and properties of fractional operators used in this paper are recalled [48].

Definition 1. The Riemann–Liouville fractional integral operator of order $\nu > 0$ of a function $u(t)$, is defined as

$$\begin{aligned} &I^{\nu}u(t) = \frac{1}{\Gamma(\nu)}\int_0^t (t-s)^{\nu-1}\, u(s)\, ds, \qquad \nu > 0, \quad t > 0, \\ &I^0 u(t) = u(t), \end{aligned} \tag{1}$$

where $\Gamma(\alpha)$ is the Gamma function defined as

$$\Gamma(\alpha) = \int_0^{\infty} t^{\alpha-1}\, \exp(-t)\, dt, \quad Re(\alpha) > 0.$$

Definition 2. The fractional derivative operator in the Caputo sense of order $\nu > 0$ of a function $u(t)$, is given as

$$\begin{aligned} &D^{\nu}u(t) = I^{m-\nu}D^{m}u(t) = \frac{1}{\Gamma(m-\nu)}\int_0^t (t-s)^{m-\nu-1}\frac{d^m}{ds^m}u(s)\,ds,\ m-1<\nu\leqslant m,\ t>0,\\ &D^0u(t) = u(t). \end{aligned} \tag{2}$$

Some properties of the operators I^{ν} and D^{ν} are recalled as follows:

1. $I^{\nu_1}I^{\nu_2}u(t) = I^{\nu_1+\nu_2}u(t)$,
2. $I^{\nu}(\lambda_1\,u_1(t)+\lambda_2\,u_2(t)) = \lambda_1\,I^{\nu}u_1(t)+\lambda_2\,I^{\nu}u_2(t)$,
3. $I^{\nu}t^{\gamma} = \frac{\Gamma(\gamma+1)}{\Gamma(\nu+\gamma+1)}t^{\nu+\gamma}, \qquad \gamma > -1$,
4. $D^{\nu}I^{\nu}u(t) = u(t)$,
5. $I^{\nu}D^{\nu}u(t) = u(t) - \sum\limits_{k=0}^{m-1}\frac{u^{(k)}(0^+)}{k!}t^k, \qquad m-1<\nu\leqslant m$,
6. $D^{\nu}t^{\gamma} = \begin{cases} 0, & \nu>\gamma,\\ \frac{\Gamma(\gamma+1)}{\Gamma(\gamma-\nu+1)}t^{\gamma-\nu}, & \text{otherwise,}\end{cases}$
7. $D^{\nu}\lambda = 0, \quad \lambda\in\mathbb{R}$,

where $\nu, \nu_1, \nu_2, \gamma, \lambda, \lambda_1, \lambda_2 \in \mathbb{R}$.

3 Existence and uniqueness of solution

In this section, we explore various forms of integro-differential equations involving fractional derivatives of arbitrary order. To investigate the existence of unique solutions and the convergence of our proposed methodology, we analyze the following FIDE:

$$D^{\nu}y(t)+h(t)\,y(t)+\int_0^t k(t,s)\,y(s)\,ds+\int_0^t \tilde{k}(t,s)\,D^{\gamma}y(s)\,ds = f(t), \qquad 0\leqslant t\leqslant 1, \tag{3}$$

where $0<\gamma<\nu$, $f(t)$, $h(t)$, $k(t,s)$, and $\tilde{k}(t,s)$, $t,s\in[0,1]$, are continuous real functions, and the proper initial conditions $y^{(i)}(0) = d_i$, $i = 0,1,\dots,m-1$ exist, where $m-1<\nu\leqslant m$.

In this section, the existence of a solution of (3) is established using the fixed point theorem. Let Y be a Banach space and let $C(J,Y)$ be the

Banach space of continuous function $y(t) \in Y$, $t \in J = [0,1]$, with the norm $\|y\| = \max\limits_{t\in J} |y(t)|$. Moreover, suppose that $B_r(y, Y)$ is a closed ball with center at y and radius r in Y. By applying the fractional integral operator, (3) will be converted to the following integral equation:

$$\begin{aligned} y(t) = F(t) &- \frac{1}{\Gamma(\nu)} \int_0^t (t-s)^{\nu-1} h(s)\, y(s)\; ds - \frac{1}{\Gamma(\nu)} \int_0^t (t-s)^{\nu-1} \int_0^s k(s,s')\, y(s')\, ds'\, ds \\ &- \frac{1}{\Gamma(\nu)} \int_0^t (t-s)^{\nu-1} \int_0^s \tilde{k}(s,s')\, D^{\gamma} y(s')\, ds'\, ds, \end{aligned} \tag{4}$$

where

$$F(t) = \sum_{i=0}^{m-1} \frac{d_i\, t^i}{\Gamma(i+1)} + \frac{1}{\Gamma(\nu)} \int_0^t (t-s)^{\nu-1} f(s)\, ds.$$

Now, suppose that for any given function $y(t) \in Y$ and kernels $k(t,s), \tilde{k}(t,s)$, there exist positive constants $L, M, \widetilde{M} \in \mathbb{R}$ such that the following conditions are satisfied:

$$\begin{aligned} &\|D^{\gamma} y(t)\| \leqslant L\ \|y(t)\|, \quad \text{for all } t \in J, \\ &\|k(t,s)\| \leqslant M, \qquad \|\tilde{k}(t,s)\| \leqslant \widetilde{M}, \quad \text{for all } (t,s) \in J \times J. \end{aligned} \tag{5}$$

Following theorem states the existence of a solution of (3).

Theorem 1. Suppose that $\nu > 0 \in \mathbb{R}$, that conditions (5) hold, and that $\|h\|/\Gamma(\nu+1) + (M + \widetilde{M}L)/\Gamma(\nu+2) < 1/2$, where $\|h\| = \max\limits_{t\in J} |h(t)|$. Then, fractional-order integro-differential equation (3) has a unique solution.

Proof. Let $W = C(J, Y)$, and define a mapping $\Psi y(t) : W \longrightarrow W$, as follows:

$$\begin{aligned} \Psi y(t) = F(t) &- \frac{1}{\Gamma(\nu)} \int_0^t (t-s)^{\nu-1} h(s)\, y(s)\; ds - \frac{1}{\Gamma(\nu)} \int_0^t (t-s)^{\nu-1} \int_0^s k(s,s')\, y(s')\, ds'\, ds \\ &- \frac{1}{\Gamma(\nu)} \int_0^t (t-s)^{\nu-1} \int_0^s \tilde{k}(s,s')\, D^{\gamma} y(s')\, ds'\, ds. \end{aligned}$$

It should be shown that Ψ has a fixed point and this fixed point is a solution of (3). Set $r \geqslant 2\|F\|$, where $\|F\| = \max\limits_{t\in J} |F(t)|$. Then, it can be shown that $\Psi B_r \subseteq B_r$, where $B_r = \{y(t) \in W |\ \|y\| \leqslant r\}$. So, one has

$$\begin{aligned} ||\Psi y(t)|| \leqslant ||F|| &+ \frac{||h||}{\Gamma(\nu)} \int_0^t (t-s)^{\nu-1} ||y(s)||\, ds \\ &+ \frac{1}{\Gamma(\nu)} \int_0^t (t-s)^{\nu-1} \int_0^s ||k(s,s')||\, ||y(s')||\, ds'\, ds \end{aligned}$$

$$
\begin{aligned}
&+\frac{1}{\Gamma(\nu)}\int_0^t (t-s)^{\nu-1}\int_0^s ||\tilde{k}(s,s')||\,||D^\gamma y(s')||\,ds'\,ds \\
&\leqslant ||F|| + \frac{||h||\,r}{\nu\,\Gamma(\nu)} + \frac{M\,r}{\nu(\nu+1)\;\Gamma(\nu)} + \frac{\widetilde{M}\,L\,r}{\nu(\nu+1)\,\Gamma(\nu)} \\
&= ||F|| + \frac{||h||\,r}{\Gamma(\nu+1)} + \frac{M\;r}{\Gamma(\nu+2)} + \frac{\widetilde{M}\,L\,r}{\Gamma(\nu+2)} \\
&\leqslant r.
\end{aligned}
$$

Thus, Ψ maps B_r into itself. Now, for $y_1(t), y_2(t) \in W$, one has

$$
\begin{aligned}
||\Psi y_1(t) - \Psi y_2(t)|| \leqslant\; & \frac{||h||}{\Gamma(\nu)}\int_0^t (t-s)^{\nu-1}||y_1(s)-y_2(s)||\,ds \\
&+ \frac{M}{\Gamma(\nu)}\int_0^t (t-s)^{\nu-1}\int_0^s ||y_1(s')-y_2(s')||\,ds'\,ds \\
&+ \frac{\widetilde{M}}{\Gamma(\nu)}\int_0^t (t-s)^{\nu-1}\int_0^s ||D^\gamma(y_1(s')-y_2(s'))||\,ds'\,ds \\
\leqslant\; & \left(\frac{||h||}{\Gamma(\nu+1)} + \frac{M+\widetilde{M}L}{\Gamma(\nu+2)}\right)||y_1(t)-y_2(t)||.
\end{aligned}
$$

Since $||h||/\Gamma(\nu+1) + (M+\widetilde{M}L)/\Gamma(\nu+2) < 1/2$, the mapping Ψ is a contraction one, and therefore a unique fixed point $y(t) \in B_r$ exists such that $\Psi y(t) = y(t)$. □

4 Shifted Jacobi polynomials and their operational matrices

The shifted Jacobi polynomials are defined on the interval $[0,1]$, with the weight function $w^{(\alpha,\beta)}(t) = t^\beta(1-t)^\alpha$. These polynomials can be determined by the following recursive relation [47]:

$$
P_{i+1}^{(\alpha,\beta)}(t) = A(\alpha,\beta,i)\,P_i^{(\alpha,\beta)}(t) + (2t-1)\,B(\alpha,\beta,i)\,P_i^{(\alpha,\beta)}(t) - C(\alpha,\beta,i)\,P_{i-1}^{(\alpha,\beta)}(t),\; i=1,2,\ldots, \tag{6}
$$

where

$$
\begin{aligned}
A(\alpha,\beta,i) &= \frac{(2i+\alpha+\beta+1)(\alpha^2-\beta^2)}{2(i+1)(i+\alpha+\beta+1)(2i+\alpha+\beta)}, \\
B(\alpha,\beta,i) &= \frac{(2i+\alpha+\beta+2)(2i+\alpha+\beta+1)}{2(i+1)(i+\alpha+\beta+1)},
\end{aligned}
$$

$$C(\alpha,\beta,i) = \frac{(i+\alpha)(i+\beta)(2i+\alpha+\beta+2)}{(i+1)(i+\alpha+\beta+1)(2i+\alpha+\beta)},$$

and

$$P_0^{(\alpha,\beta)}(t) = 1, \quad P_1^{(\alpha,\beta)}(t) = \frac{\alpha+\beta+2}{2}(2t-1) + \frac{\alpha-\beta}{2}.$$

In addition, these shifted polynomials are orthogonal, that is,

$$\int_0^1 P_i^{(\alpha,\beta)}(t)\, P_j^{(\alpha,\beta)}(t)\, w^{(\alpha,\beta)}(t)\, dt = h_i\ \delta_{ij},$$

where

$$h_i = \frac{\Gamma(i+\alpha+1)\Gamma(i+\beta+1)}{(2i+\alpha+\beta+1)\, i!\, \Gamma(i+\alpha+\beta+1)},$$

and δ_{ij} denotes the Kronecker delta function. Moreover, the shifted Jacobi polynomials have the following power series presentation, which will be used throughout this research:

$$P_i^{(\alpha,\beta)}(t) = \sum_{k=0}^{i} \frac{(-1)^{i-k}\Gamma(i+\beta+1)\Gamma(i+k+\alpha+\beta+1)\, t^k}{\Gamma(k+\beta+1)\Gamma(i+\alpha+\beta+1)\,(i-k)!\,k!}, \qquad i = 0, 1, \ldots. \tag{7}$$

A square integrable function $u(t)$, in the interval $[0,1]$, can be expressed in terms of shifted Jacobi polynomials as the following equation:

$$u(t) = \sum_{j=0}^{\infty} \hat{u}_j\, P_j^{(\alpha,\beta)}(t), \tag{8}$$

where the coefficients $\hat{u}_j$ are given by

$$\hat{u}_j = \frac{1}{h_j}\int_0^1 u(t)\, P_j^{(\alpha,\beta)}(t)\, w^{(\alpha,\beta)}(t)\, dt, \qquad j = 0, 1, \ldots.$$

In practice, only the first $(N+1)$ terms of the shifted Jacobi polynomials are considered. Therefore, we have

$$u(t) \approx u_N(t) = \sum_{j=0}^{N} \hat{u}_j\, P_j^{(\alpha,\beta)}(t) = \Phi^T(t)\,\hat{U} = \hat{U}^T\, \Phi(t), \tag{9}$$

where the vectors $\hat{U}$ and $\Phi(t)$ are given by

$$\hat{U} = [\hat{u}_0, \hat{u}_1, \ldots, \hat{u}_N]^T, \qquad \Phi(t) = [P_0^{(\alpha,\beta)}(t), P_1^{(\alpha,\beta)}(t), \ldots, P_N^{(\alpha,\beta)}(t)]^T. \tag{10}$$

Similarly, any continuous two-variable function, say $g(t,s)$, defined on $[0,1]\times[0,1]$, can be expanded as follows in terms of the double-shifted Jacobi polynomials:

$$g_N(t,s)=\sum_{i=0}^{N}\sum_{j=0}^{N} g_{ij}\, P_i^{(\alpha,\beta)}(t)\, P_j^{(\alpha,\beta)}(s)=\Phi^T(t)\, G\, \Phi(s),$$

where G is a $(N+1)\times(N+1)$ matrix and its entries are given by

$$g_{ij}=\frac{1}{h_i\, h_j}\int_0^1\int_0^1 g(t,s)\, P_i^{(\alpha,\beta)}(t)\, P_j^{(\alpha,\beta)}(s)\, w^{(\alpha,\beta)}(t)\, w^{(\alpha,\beta)}(s)\, dt\, ds,\ \ i,j=0,1,\ldots,N. \quad (11)$$

The following relations hold for the shifted Jacobi polynomials:

(i) $P_i^{(\alpha,\beta)}(0)=(-1)^i\binom{i+\beta}{i}$,

(ii) $\frac{d^i P_n^{(\alpha,\beta)}(t)}{dt^i}=\frac{\Gamma(n+i+\alpha+\beta+1)}{\Gamma(n+\alpha+\beta+1)}P_{n-i}^{(\alpha+i,\beta+i)}(t), \quad i=0,1,\ldots.$

4.1 The Jacobi operational matrices

In implementing operations on the Jacobi basis, we frequently encounter the integration of the vector $\Phi(t)$ defined in (10), as well as the need to evaluate the product of two vectors, $\Phi(t)$ and $\Phi^T(t)$ (the product matrix). To address this, we will derive the corresponding operational matrices. To proceed, some lemmas regarding the shifted Jacobi polynomials are necessary. These are as follows:

Lemma 1. The shifted Jacobi polynomial $P_i^{(\alpha,\beta)}(t)$, $t\in[0,1]$, can be presented in the form

$$P_i^{(\alpha,\beta)}(t)=\sum_{j=0}^{i}\gamma_j^{(i)}\, t^j, \quad i=0,1,\ldots,$$

where the coefficients $\gamma_j^{(i)}$ are calculated as

$$\gamma_j^{(i)}=(-1)^{i-j}\binom{i+j+\alpha+\beta}{j}\binom{i+\beta}{i-j}.$$

Proof. The coefficients $\gamma_j^{(i)}$ can be obtained as

$$\gamma_j^{(i)} = \frac{1}{j!}\frac{d^j}{dt^j}\, P_i^{(\alpha,\beta)}(t)\Big|_{t=0}.$$

Now, using the relations (i) and (ii) stated in the above, the lemma can be proved. □

Lemma 2. If $i \in \mathbb{N}$ and $l \geqslant i$, then

$$\int_0^1 t^l\, P_i^{(\alpha,\beta)}(t)\, w^{(\alpha,\beta)}(t)\, dt$$
$$= \sum_{k=0}^{i} \frac{(-1)^{i-k}\,\Gamma(i+\beta+1)\,\Gamma(i+k+\alpha+\beta+1)\,\Gamma(l+k+\beta+1)\,\Gamma(\alpha+1)}{\Gamma(k+\beta+1)\,\Gamma(i+\alpha+\beta+1)\,\Gamma(l+k+\alpha+\beta+2)\,(i-k)!\,k!}.$$

Proof. The lemma can be easily proved by integrating of (7). □

In FIDEs, such as (3), one of the derivative orders, either ν or γ, may be an integer. Therefore, both the operational matrices for the integration of integer and fractional orders need to be applied to approximate the main equation. Specifically, the integral operational matrix of integer order is used to approximate the integral component of the given equation. As a result, Jacobi operational matrices for integration are derived for both cases. The entries of these matrices are computed using the following theorems.

Theorem 2. Let $\Phi(t)$ be the Jacobi vector in (10) and $\nu \in \mathbb{R}$. Then, one has

$$I^{\nu}\Phi(t) \approx \mathbf{P}^{(\nu)}\,\Phi(t),$$

where I^{ν} is the Riemann–Liouville fractional integral operator of order ν and $\mathbf{P}^{(\nu)}$ is the $(N+1)\times(N+1)$ fractional operational matrix of integration and is defined by

$$\mathbf{P}^{(\nu)} = \begin{bmatrix} \theta(0,0) & \theta(0,1) & \dots & \theta(0,N) \\ \theta(1,0) & \theta(1,1) & \dots & \theta(1,N) \\ \vdots & \vdots & \ddots & \vdots \\ \theta(N,0) & \theta(N,1) & \dots & \theta(N,N) \end{bmatrix},$$

where

$$\theta(i,j) = \sum_{k=0}^{i} \omega'_{ijk}, \qquad i = 0,1,\dots,N, \quad j = 1,2,\dots,N, \tag{12}$$

and ω'_{ijk} are given by

$$\omega'_{ijk}=\frac{(-1)^{i-k}\ \Gamma(j+\beta+1)\ \Gamma(i+\beta+1)\ \Gamma(i+k+\alpha+\beta+1)\ \Gamma(\alpha+1)}{h_j\ \Gamma(j+\alpha+\beta+1)\ \Gamma(k+\beta+1)\ \Gamma(i+\alpha+\beta+1)\ \Gamma(k+\nu+1)\ (i-k)!}$$
$$\times\sum_{l=0}^{j}\frac{(-1)^{j-l}\ \Gamma(j+l+\alpha+\beta+1)\ \Gamma(l+k+\nu+\beta+1)}{\Gamma(l+\beta+1)\ \Gamma(l+k+\nu+\alpha+\beta+2)\ l!(j-l)!},\quad i,j=0,1,\dots,N.$$

Proof. Applying fractional integral operator (1) to relation (7) leads to

$$I^{\nu}P_i^{(\alpha,\beta)}(t)=\sum_{k=0}^{i}\frac{(-1)^{i-k}\ \Gamma(i+\beta+1)\ \Gamma(i+k+\alpha+\beta+1)\ t^{k+\nu}}{\Gamma(k+\beta+1)\ \Gamma(i+\alpha+\beta+1)\ \Gamma(k+\nu+1)\ (i-k)!}. \tag{13}$$

Moreover, $t^{k+\nu}$ can be approximated in terms of the shifted Jacobi polynomials as the following form:

$$t^{k+\nu}\approx\sum_{j=0}^{N}a_{k,j}\ P_j^{(\alpha,\beta)}(t),$$

where

$$a_{k,j}=\frac{1}{h_j}\int_0^1 t^{k+\nu}\ P_j^{(\alpha,\beta)}(t)\ w^{(\alpha,\beta)}(t)\ dt.$$

According to Lemma 2, (13) can be rewritten as

$$\begin{aligned}
&I^{\nu}P_i^{(\alpha,\beta)}(t)\\
&\approx\sum_{j=0}^{N}\left\{\sum_{k=0}^{i}\frac{(-1)^{i-k}\ \Gamma(j+\beta+1)\ \Gamma(i+\beta+1)\ \Gamma(i+k+\alpha+\beta+1)\ \Gamma(\alpha+1)}{h_j\ \Gamma(j+\alpha+\beta+1)\ \Gamma(k+\beta+1)\ \Gamma(i+\alpha+\beta+1)\ \Gamma(k+\nu+1)\ (i-k)!}\right.\\
&\left.\times\sum_{l=0}^{j}\frac{(-1)^{j-l}\ \Gamma(j+l+\alpha+\beta+1)\ \Gamma(l+k+\nu+\beta+1)}{\Gamma(l+\beta+1)\ \Gamma(l+k+\nu+\alpha+\beta+2)\ l!(j-l)!}\right\}P_j^{(\alpha,\beta)}(t)\\
&=\sum_{j=0}^{N}\ \theta(i,j)\ P_j^{(\alpha,\beta)}(t),
\end{aligned}$$

where $\theta(i,j)$ are given in (12). Rewriting the last relation as a vector form gives

$$I^{\nu}P_i^{(\alpha,\beta)}(t)=[\theta(i,0),\theta(i,1),\dots,\theta(i,N)]\ \Phi(t),\qquad i=0,1,\dots,N.$$

This leads to the desired result. □

Theorem 3. Let $\Phi(t)$ be the Jacobi vector in (10). Then,

$$\int_0^t\Phi(t')\ dt'\approx\mathbf{P}\ \Phi(t),$$

where $\mathbf{P}$ is the $(N+1)\times(N+1)$ operational matrix of integration (of integer order) and is defined by

$$\mathbf{P}=\begin{bmatrix} \pi(0,0) & \pi(0,1) & \dots & \pi(0,N) \\ \pi(1,0) & \pi(1,1) & \dots & \pi(1,N) \\ \vdots & \vdots & \ddots & \vdots \\ \pi(N,0) & \pi(N,1) & \dots & \pi(N,N) \end{bmatrix},$$

where

$$\pi(i,j)=\sum_{k=0}^{i}\omega_{ijk}, \qquad i,j=0,1,\dots,N, \tag{14}$$

and ω_{ijk} are given by

$$\omega_{ijk}=\frac{(-1)^{i-k}\ \Gamma(j+\beta+1)\ \Gamma(i+\beta+1)\ \Gamma(i+k+\alpha+\beta+1)\ \Gamma(\alpha+1)}{h_j\ \Gamma(j+\alpha+\beta+1)\ \Gamma(k+\beta+1)\ \Gamma(i+\alpha+\beta+1)\ (k+1)!\ (i-k)!}$$
$$\times\sum_{l=0}^{j}\frac{(-1)^{j-l}\ \Gamma(j+l+\alpha+\beta+1)\ \Gamma(l+k+\beta+2)}{\Gamma(l+\beta+1)\ \Gamma(l+k+\alpha+\beta+3)\ l!(j-l)!}, \quad i,j=0,1,\dots,N.$$

Proof. The proof is almost the same as that presented in Theorem 2. By setting $\nu=1$, in the proof of Theorem 2, the matrix $\mathbf{P}$ will be obtained. □

In the following, some useful and applicable lemmas are presented to obtain the Jacobi operational matrix of the product.

Lemma 3. If $P_j^{(\alpha,\beta)}(t)$ and $P_k^{(\alpha,\beta)}(t)$ are, respectively, jth and kth shifted Jacobi polynomials, then the product of $P_j^{(\alpha,\beta)}(t)$ and $P_k^{(\alpha,\beta)}(t)$ can be written as

$$Q_{j+k}^{(\alpha,\beta)}(t)=P_j^{(\alpha,\beta)}(t)P_k^{(\alpha,\beta)}(t)=\sum_{r=0}^{j+k}\lambda_r^{(j,k)}\ t^r,$$

where the coefficients $\lambda_r^{(j,k)}$ are determined as follows:

The quantities $\gamma_l^{(k)}$ and $\gamma_{r-l}^{(j)}$ are introduced, respectively, for $P_k^{(\alpha,\beta)}(t)$ and $P_j^{(\alpha,\beta)}(t)$ based on Lemma 1.

Proof. See [45, p. 496, Lemma 3] . □

Lemma 4. If $P_i^{(\alpha,\beta)}(t)$, $P_j^{(\alpha,\beta)}(t)$, and $P_k^{(\alpha,\beta)}(t)$ are, respectively, ith, jth, and kth shifted Jacobi polynomials, then

$$q_{ijk}=\int_0^1 P_i^{(\alpha,\beta)}(t)\ P_j^{(\alpha,\beta)}(t)\ P_k^{(\alpha,\beta)}(t)\ w^{(\alpha,\beta)}(t)\ dt$$

If $j \geq k$:

$r = 0, 1, \ldots, j+k,$

if $r > j$ then

$\lambda_r^{(j,k)} = \sum_{l=r-j}^{k} \gamma_{r-l}^{(j)} \ \gamma_l^{(k)},$

else

$r_1 = \min\{r, k\},$

$\lambda_r^{(j,k)} = \sum_{l=0}^{r_1} \gamma_{r-l}^{(j)} \ \gamma_l^{(k)},$

end.

If $j < k$:

$r = 0, 1, \ldots, j+k,$

if $r \leq j$ then

$r_1 = \min\{r, j\},$

$\lambda_r^{(j,k)} = \sum_{l=0}^{r_1} \gamma_{r-l}^{(j)} \ \gamma_l^{(k)},$

else

$r_2 = \min\{r, k\},$

$\lambda_r^{(j,k)} = \sum_{l=r-j}^{r_2} \gamma_{r-l}^{(j)} \ \gamma_l^{(k)},$

end.

$$= \sum_{l=0}^{j+k} \sum_{m=0}^{i} \frac{(-1)^{i-m} \lambda_l^{(j,k)} \ \Gamma(i+\beta+1) \ \Gamma(i+m+\alpha+\beta+1) \ \Gamma(l+m+\beta+1) \ \Gamma(\alpha+1)}{\Gamma(m+\beta+1) \ \Gamma(i+\alpha+\beta+1) \ \Gamma(l+m+\alpha+\beta+2) \ (i-m)! \ m!},$$

where $\lambda_l^{(j,k)}$ is computed by Lemma 3.

Proof. See [46, p. 12, Lemma 5]. □

The following theorem presents a general formula for finding the $(N+1) \times (N+1)$ operational matrix of product $\widetilde{V}$ whenever

$$\Phi(t) \ \Phi^T(t) \ V \approx \widetilde{V} \ \Phi(t), \tag{15}$$

and V is a given $(N+1)$ vector.

Theorem 4. The entries of the matrix $\widetilde{V}$ in (15) are computed as follows:

$$\widetilde{V}_{jk} = \frac{1}{h_k} \sum_{i=0}^{N} V_i \ q_{ijk}, \qquad j, k = 0, 1, \ldots, N,$$

where q_{ijk} is introduced by Lemma 4 and V_i is the components of the vector V in (15).

Proof. See [46, p. 12, Theorem 2]. □

Remark 1. If $u(t) \approx U^T\ \Phi(t) = \Phi^T(t)\ U$ and $v(t) \approx V^T\ \Phi(t) = \Phi^T(t)\ V$, where U and V are $(N+1)$ vectors, using the operational matrix of product, it is easily shown that

$$\begin{aligned}
&u^2(t) \approx U^T\ \widetilde{U}\ \Phi(t),\\
&u^3(t) \approx F^T\ \widetilde{U}\ \Phi(t), \qquad F = \widetilde{U}^T\ U,\\
&u(t)\ v(t) \approx U^T\ \widetilde{V}\ \Phi(t).
\end{aligned}$$

The following remark is useful to approximate the integral parts of equations under study.

Remark 2. Let the vector $\Phi(t)$ be the shifted Jacobi vector in (10). Then

$$\mathbf{M} = \int_0^1 \Phi(t)\ \Phi^T(t)\ dt,$$

where

$$\mathbf{M}_{i,j} = \sum_{r=0}^{i+j} \frac{\lambda_r^{(i,j)}}{r+1}, \quad i,j = 0,1,\ldots,N,$$

and $\lambda_r^{(j,k)}$ is introduced by Lemma 3.

4.2 Methodology

To continue with the implementation of the proposed method, consider the following cases.

4.2.1 Case I

$$\begin{aligned}
D^{\nu} y(t) + h(t)\ y(t) + \int_0^t k(t,s)\ y(s)\ ds&\\
+ \int_0^t \tilde{k}(t,s)\ D^{\gamma} y(s)\ ds = f(t),& \qquad 0 \leqslant t \leqslant 1, \quad 0 < \gamma < \nu \leqslant m, \qquad (16)
\end{aligned}$$

with initial conditions,

$$y^{(j)}(0) = d_j, \qquad j = 0, 1, \ldots, m-1,$$

$h(t)$, $k(t,s)$, and $\tilde{k}(t,s)$ are known continuous functions. Since $D^{\nu}y(t)$ has the highest order of derivative in (16), it can be approximated as

$$D^{\nu}y(t) \approx \Phi^T(t)\ C, \tag{17}$$

where the vectors $\Phi(t)$ is defined by (10) and $C = [c_0, c_1, \ldots, c_N]$ is the vector of unknown coefficients. By applying the fractional integral operator of order ν to (17), an approximation of unknown function $y(t)$ is resulted as follows:

$$\begin{aligned} y(t) &\approx \Phi^T(t)\ \mathbf{P}^{(\nu)\mathbf{T}}\ C + \sum_{j=0}^{m-1} \frac{d_j\ t^j}{j!} \\ &\approx \Phi^T(t)\ \mathbf{P}^{(\nu)\mathbf{T}}\ C + \Phi^T(t)\ F_1, \end{aligned} \tag{18}$$

where F_1 is a known $(N+1)$ vector and computed as

$$\sum_{j=0}^{m-1} \frac{d_j\ t^j}{j!} \approx \Phi^T(t) F_1,$$

$$(F_1)_k = \frac{1}{h_k} \sum_{j=0}^{m-1} \frac{d_j}{j!} \int_0^1 t^j\ P_k^{(\alpha,\beta)}(t) w^{(\alpha,\beta)}(t) dt, \qquad k = 0, 1, \ldots, N.$$

Now, using approximation (17), the following steps can be pursued to approximate the term $D^{\gamma}y(t)$, $\gamma < \nu$:

$$D^{\nu}y(t) = D^{\nu-\gamma}D^{\gamma}\ y(t) \approx \Phi^T(t)\ C.$$

Applying the fractional integral operator of order $\nu - \gamma$ on both sides of the last approximation yields the following approximation:

$$\begin{aligned} D^{\gamma}\ y(t) &\approx \Phi^T(t)\ \mathbf{P}^{(\nu-\gamma)\mathbf{T}}\ C + \sum_{j=\lceil \gamma \rceil}^{m-1} \frac{d_j\ t^{j-\gamma}}{\Gamma(j-\gamma+1)} \\ &\approx \Phi^T(t)\ \mathbf{P}^{(\nu-\gamma)\mathbf{T}}\ C + \Phi^T(t)\ F_2, \end{aligned} \tag{19}$$

where

$$\sum_{j=\lceil\gamma\rceil}^{m-1} \frac{d_j\ t^{j-\gamma}}{\Gamma(j-\gamma+1)} \approx \Phi^T(t)F_2,$$

$$(F_2)_k = \frac{1}{h_k} \sum_{j=\lceil\gamma\rceil}^{m-1} \frac{d_j}{\Gamma(j-\gamma+1)} \int_0^1 t^{j-\gamma}\ P_k^{(\alpha,\beta)}(t) w^{(\alpha,\beta)}(t)dt, \qquad k = 0,1,\dots,N.$$

The kernels of integral parts, $k(t,s)$ and $\tilde{k}(t,s)$, are approximated as follows by means of (11):

$$k(t,s) \approx \Phi^T(t)\ K\ \Phi(s), \qquad \tilde{k}(t,s) \approx \Phi^T(t)\ \widetilde{K}\ \Phi(s),$$

where K and $\widetilde{K}$ are the known $(N+1)\times(N+1)$ matrices. Using the introduced matrices, the integral parts of (16) are approximated as follows:

$$\begin{aligned}\int_0^t k(t,s)\ y(s)\ ds &\approx \int_0^t \Phi^T(t)\ K\ \Phi(s)\ \Phi^T(s)\ U_1\ ds \\ &\approx \Phi^T(t)\ K \int_0^t \Phi(s)\ \Phi^T(s)\ U_1\ ds \\ &= \Phi^T(t)\ K\ \widetilde{U}_1\ \mathbf{P}\ \Phi(t), \qquad U_1 = \mathbf{P}^{(\nu)\mathbf{T}}\ C + F_1, \\ \int_0^t \tilde{k}(t,s)\ D^\gamma\ y(s)\ ds &\approx \Phi^T(t)\ \widetilde{K}\ \widetilde{U}_2\ \mathbf{P}\ \Phi(t), \qquad U_2 = \mathbf{P}^{(\nu-\gamma)\mathbf{T}}\ C + F_2,\end{aligned} \tag{20}$$

where $\widetilde{U}_1, \widetilde{U}_2$ are operational matrices of product, corresponding to the vectors U_1, U_2, respectively. In this way, the unknown function and its derivatives are approximated after substituting approximations (17)–(20) into (16), the main equation is converted into the following algebraic equation:

$$\Phi^T(t)\ C + h(t)\ \Phi^T(t)\ U_1 + \Phi^T(t)\ K\ \widetilde{U}_1\ \mathbf{P}\ \Phi(t) + \Phi^T(t)\ \widetilde{K}\ \widetilde{U}_2\ \mathbf{P}\ \Phi(t) - f(t) \approx 0. \tag{21}$$

Lemma 5. Let $y_N(t)$ be the approximate solution obtained from the proposed scheme, and let $y(t)$ be the exact solution to (16). Suppose that $0 < \|h\|\Gamma(\nu+1) + \frac{M+\widetilde{M}}{\Gamma(\nu+2)} < 1$, where $\tilde{y}(t)$ represents the error of $y_N(t)$, and $\mathcal{H}_N(t)$ is the perturbation term. Then, the following equation holds:

$$\|\tilde{y}\| \leq \Lambda^*\ \|\mathcal{H}_n\|,$$

where Λ^* is a positive constant.

Proof. As can be seen, applying the Riemann–Liouville integral operator to (16) results in (3). it is clear that $y_N(t)$ and $y_N(t)+\tilde{y}(t)$ satisfy the following equations:

$$\begin{aligned} y_N(t) = F(t) + \mathcal{H}_N(t) - \frac{1}{\Gamma(\nu)}\int_0^t (t-s)^{\nu-1} h(s) y_N(s)\, ds \\ - \frac{1}{\Gamma(\nu)}\int_0^t (t-s)^{\nu-1}\int_0^s k(s,r) y_N(r)\, dr\, ds \\ - \frac{1}{\Gamma(\nu)}\int_0^t (t-s)^{\nu-1}\int_0^s \tilde{k}(s,r) D^\gamma y_N(r)\, dr\, ds, \end{aligned} \tag{22}$$

$$\begin{aligned} y_N(t) + \tilde{y}(t) = F(t) - \frac{1}{\Gamma(\nu)}\int_0^t (t-s)^{\nu-1} h(s)(y_N(s)+\tilde{y}(s))\, ds \\ - \frac{1}{\Gamma(\nu)}\int_0^t (t-s)^{\nu-1}\int_0^s k(s,r)(y_N(r)+\tilde{y}(r))\, dr\, ds \\ - \frac{1}{\Gamma(\nu)}\int_0^t (t-s)^{\nu-1}\int_0^s \tilde{k}(s,r) D^\gamma (y_N(r)+\tilde{y}(r))\, dr\, ds, \end{aligned} \tag{23}$$

where

$$F(t) = \sum_{i=0}^{m-1} \frac{d_i\, t^i}{\Gamma(i+1)} + \frac{1}{\Gamma(\nu)}\int_0^t (t-s)^{\nu-1} f(s)\, ds.$$

Subtracting (22) from (23) leads to the following equation:

$$\begin{aligned} \tilde{y}(t) = -\frac{1}{\Gamma(\nu)}\int_0^t (t-s)^{\nu-1} h(s)(y_N(s)+\tilde{y}(s))\, ds \\ - \frac{1}{\Gamma(\nu)}\int_0^t (t-s)^{\nu-1}\int_0^s k(s,r)(y_N(r)+\tilde{y}(r))\, dr\, ds \\ - \frac{1}{\Gamma(\nu)}\int_0^t (t-s)^{\nu-1}\int_0^s \tilde{k}(s,r) D^\gamma (y_N(r)+\tilde{y}(r))\, dr\, ds. \end{aligned} \tag{24}$$

Taking the norm from (24) yields the following inequality:

$$\begin{aligned} \|\tilde{y}\| &\leq \|\mathcal{H}_N\| + \frac{\|h\|\,\|\tilde{y}\|}{\Gamma(\nu)}\int_0^t (t-s)^{\nu-1} ds + \frac{M\,\|\tilde{y}\|}{\Gamma(\nu)}\int_0^t (t-s)^{\nu-1} ds + \frac{\widetilde{M}\,L\,\|\tilde{y}\|}{\Gamma(\nu)}\int_0^t (t-s)^{\nu-1} ds \\ &\leq \mathcal{H}_N\| + \frac{\|h\|\,\|\tilde{y}\|}{\Gamma(\nu+1)} + fracM\,\|\tilde{y}\|\Gamma(\nu+2) + \frac{\widetilde{M}\,L\,\|\tilde{y}\|}{\Gamma(\nu+2)}. \end{aligned}$$

Since $0 < \|h\|\Gamma(\nu+1) + (M+\widetilde{M})/\Gamma(\nu+2) < 1$, so one has

$$\|\tilde{y}\| \leq \frac{1}{1 - \frac{\|h\|}{\Gamma(\nu+1)} - \frac{M+\widetilde{M}}{\Gamma(\nu+2)}}\|\mathcal{H}_N\|,$$

and the desired result is acquired.

Thus, the variation of the approximate solution is bounded. Since the existence and uniqueness of the given equation have already been established in section 3, it follows that (16) is well-posed. □

4.2.2 Case II

$$y''(t) + h(t)\ y'(t) + g(t)\ D^{\nu}y(t) + \int_0^t k(t,s)\ y(s)\ ds = f(t),\ 0 \leqslant t \leqslant 1,\ 0 < \nu < 2, \quad (25)$$

subject to initial conditions

$$y^{(j)}(0) = d_j, \qquad j = 0, 1,$$

where $h(t)$, $g(t)$, $k(t,s)$, and $\tilde{k}(t,s)$ are known continuous functions. Since $y''(t)$ has the highest order of derivative in (25), successive integrating leads to the following approximations:

$$\begin{aligned} &y''(t) \approx \Phi^T(t)\ C, \\ &y'(t) \approx \Phi^T(t)\ \mathbf{P}^T\ C + \Phi^T(t)\ F_1, \qquad d_1 \approx \Phi^T(t)\ F_1, \\ &y(t) \approx \Phi^T(t)\ (\mathbf{P}^T)^2\ C + \Phi^T(t)\ \mathbf{P}^T\ F_1 + \Phi^T(t)\ F_2, \qquad d_0 \approx \Phi^T(t)\ F_2, \end{aligned} \quad (26)$$

where $\mathbf{P}$ is the operational matrix of integration of integer order, as introduced in Theorem 3. To approximate $D^{\nu}y(t)$, where $\nu \in \mathbb{R}$ is a noninteger value, the first approximation in (26) can be used as follows:

$$D^2y(t) = D^{2-\nu}D^{\nu}y(t) \approx \Phi^T(t)\ C.$$

So,

$$\begin{aligned} D^{\nu}y(t) &\approx \Phi^T(t)\ \mathbf{P}^{\mathbf{(2-\nu)T}}\ C + \sum_{i=\lceil \nu \rceil}^{m-1} \frac{d_i\ t^{i-\nu}}{\Gamma(i-\nu+1)} \\ &\approx \Phi^T(t)\ \mathbf{P}^{\mathbf{(2-\nu)T}}\ C + \Phi^T(t)\ F_3, \qquad m-1 < \nu \leqslant m, \end{aligned} \quad (27)$$

where $\mathbf{P}^{\mathbf{(2-\nu)}}$ is the operational matrix of fractional integration related to the fractional integral operator of order $2-\nu$. The integral part of (25) is converted to the following algebraic approximation:

$$\int_0^t k(t,s)\ y(s)\ ds \approx \Phi^T(t)\ K\ \widetilde{U}\ \mathbf{P}\ \Phi(t), \qquad U = (\mathbf{P}^T)^2\ C + \mathbf{P}^T\ F_1 + F_2, \tag{28}$$

where $\widetilde{U}$ is the operational matrix of product, corresponding to the vector U. Substituting the approximations (26)–(28) into (25) yields the following algebraic equation:

$$\Phi^T(t)\ C + h(t)\ \Phi^T(t)\{\mathbf{P}^T\ C + F_1\} + g(t)\ \Phi^T(t)\{\mathbf{P}^{(2-\nu)}T\ C + F_3\} + \Phi^T(t)\ K\ \widetilde{U}\ \mathbf{P}\ \Phi(t) - f(t) \approx 0. \tag{29}$$

4.2.3 Case III

$$D^\nu y(t) + h(t)\ y(t) + \lambda_1 \int_0^t k(t,s)\ y^2(s)\ ds + \lambda_2 \int_0^1 \tilde{k}(t,s)\ y^2(s)\ ds = f(t), \quad 0 \leqslant t \leqslant 1, \quad \nu \in \mathbb{R}, \tag{30}$$

subject to initial conditions

$$y^{(j)}(0) = d_j, \qquad j = 0, 1, \dots, m-1,$$

where $\lambda_1, \lambda_2 \in \mathbb{R}$ and $h(t)$, $k(t,s)$, and $\tilde{k}(t,s)$ are known continuous functions. Following the process the same as for the last two cases, leads to the approximations below:

$$\begin{aligned}
&D^\nu y(t) \approx \Phi^T(t)\ C, \qquad y(t) \approx \Phi^T(t)\ \mathbf{P}^{(\nu)\mathbf{T}}\ C + \Phi^T(t)\ F_1 = \Phi^T(t)\ U,\\
&y^2(t) \approx U^T\ \widetilde{U}\ \Phi(t) = \Phi^T(t)\ F_2, \qquad \int_0^t k(t,s)\ y^2(s)\ ds \approx \Phi^T(t)\ K\ \widetilde{F}_2\ \mathbf{P}\ \Phi(t),\\
&\int_0^1 \widetilde{k}(t,s)\ y^2(s)\ ds \approx \Phi^T(t)\ \widetilde{K}\ \mathbf{M}\ \widetilde{F}_2,
\end{aligned} \tag{31}$$

where $\mathbf{M}$ is the matrix introduced by Remark 2. Substituting the approximations (31) into (30) yields the following algebraic equation:

$$\Phi^T(t)\ C + h(t)\ \Phi^T(t)\ U + \lambda_1 \Phi^T(t)\ K\ \widetilde{F}_2\ \mathbf{P}\ \Phi(t) + \lambda_2 \Phi^T(t)\ \widetilde{K}\ \mathbf{M}\ F_2 - f(t) \approx 0. \tag{32}$$

The resulting algebraic equations (21), (29), and (32) are collocated at the $(N+1)$ roots of the $(N+1)$th shifted Jacobi polynomials on the interval $[0,1]$. By solving the systems of generated algebraic equations, the unknown vector C can be determined. Thus, by selecting appropriate values for the parameters α and β, an approximate solution can be obtained using the approximation in (18), the third approximation in (26), and the second approximation in (31). The resulting nonlinear systems can be solved using the Newton iteration method.

Remark 3. Based on the discussions in this section and the statement made in Remark 2, the nonlinear terms and integral components in the equations under study are approximated in vector form. Therefore, the initial conditions of the equations must be approximated in terms of the Jacobi basis.

5 Convergence analysis and error bounds

In this section, some upper bounds are presented for the residual function and the proposed algorithm. It can be seen that the upper bounds decrease when the number of terms in the series solution increases. For this purpose, some useful definitions and theorems are stated.

The set of all algebraic polynomials of degree at most N is denoted by $\mathbb{P}_N$. The orthogonal projection $\mathcal{P}_{N,\alpha,\beta} : L^2_{w^{(\alpha,\beta)}}(J) \to \mathbb{P}_N$, $J = [0, 1]$, is considered for $u(t) \in L^2_{w^{(\alpha,\beta)}}(J)$ and defined by

$$(\mathcal{P}_{N,\alpha,\beta}u - u,\ v) = 0, \qquad \text{for all } v \in \mathbb{P}_N.$$

The Jacobi-weighted Sobolev space is introduced as

$$\mathcal{J}^r_{w^{(\alpha,\beta)}}(J) = \{u|\ \text{u is measurable and } \|u\|_{r,w^{(\alpha,\beta)}} < \infty\}, \qquad r \in \mathbb{N},$$

equipped with the following norm and semi-norm:

$$\|u\|_{r,w^{(\alpha,\beta)}} = \left(\sum_{k=0}^{r} \|\ \frac{d^k u}{dt^k}\ \|^2_{w^{(\alpha+k,\beta+k)}}\right)^{\frac{1}{2}}, \qquad |u|_{r,w^{(\alpha,\beta)}} = ||\frac{d^r u}{dt^r}||_{w^{(\alpha+r,\beta+r)}}.$$

Theorem 5. For any $u \in \mathcal{J}^r_{w^{(\alpha,\beta)}}(J)$, $r \in \mathbb{N}$, $0 \leqslant \mu \leqslant r$, one has

$$\|u - \mathcal{P}_{N,\alpha,\beta}u\|_{\mu,w^{(\alpha,\beta)}} \leqslant c(N(N + \alpha + \beta))^{\frac{\mu-r}{2}} |u|_{r,w^{(\alpha,\beta)}},$$

where c is a positive constant independent of N, α, and β.

Proof. See [17, p. 5, Theorem 2.1] . □

Corollary 1. If $k(t, s)$ is a continuous function on $J \times J$ and $k_N(t, s) = \mathcal{P}_{N,\alpha,\beta}k(t, s)$ is an approximation to $k(t, s)$ in the Jacobi-weighted Sobolev space, then the error can be bounded as follows:

$$\|k(t,s)-k_N(t,s)\|_{\mu,W^{(\alpha,\beta)}} \leqslant c_0(N(N+\alpha+\beta))^{\mu-r}|k(t,s)|_{r,W^{(\alpha,\beta)}}, \quad (33)$$

where $W^{(\alpha,\beta)}(t,s) = w^{(\alpha,\beta)}(t)w^{(\alpha,\beta)}(s)$. For more details, the interested reader is referred to . 502-5041[45].

Lemma 6. If $n \in \mathbb{N}$, $u \in \mathcal{J}^r_{w^{(\alpha,\beta)}}(J)$, and $D^n u(t)$ is the nth derivative of $u(t)$, then

$$\begin{aligned}&\|D^n u - D^n \mathcal{P}_{N,\alpha,\beta}u\|_{\mu,w^{(\alpha+n,\beta+n)}}\\ &\leqslant c^*\Big((N+n)(N+n+\alpha+\beta)\Big)^{\frac{\mu-r}{2}}|u^{(n)}|_{r,w^{(\alpha+n,\beta+n)}}, \quad 0\leqslant\mu\leqslant r. \quad (34)\end{aligned}$$

Proof. By differentiating the Jacobi series solution and applying Theorem 5, the desired result is acquired. □

Lemma 7. [Generalized Hardy's inequality [8, p. 679, Lemma 3.8]] For all measurable functions $u \geqslant 0$, the following generalized Hardy's inequality:

$$\left(\int_a^b |(Tu)(t)|^q \; w_1(t)\; dt\right)^{1/q} \leqslant \rho\left(\int_a^b |u(t)|^p \; w_2(t)\; dt\right)^{1/p},$$

holds if and only if

$$\sup_{a<t<b}\left(\int_t^b w_1(t)\; dt\right)^{1/q}\left(\int_a^t w_2^{1-p'}(t)\; dt\right)^{1/p'} < \infty,$$

where $p' = \frac{p}{p-1}$, $1 < p \leqslant q < \infty$, w_1, w_2 are weight functions, and T is an integral operator of the following form:

$$(Tu)(t) = \int_a^t \bar{k}(t,s)\; u(s)\; ds,$$

where $\bar{k}(t,s)$ is a given kernel.

Theorem 6. If $\nu, \mu \in \mathbb{R}$, $\nu > 0$, $0 \leqslant \mu \leqslant r$, and $D^\nu u(t)$ denotes the Caputo fractional derivative of $u(t) \in \mathcal{J}^r_{w^{(\alpha,\beta)}}(J)$ of order ν, then

$$\begin{aligned}&\|D^\nu u - D^\nu \mathcal{P}_{N,\alpha,\beta}u\|_{\mu,w^{(\alpha+m,\beta+m)}}\\ &\leqslant \frac{\rho\; c'}{\Gamma(m-\nu)}\Big((N+m)(N+m+\alpha+\beta)\Big)^{\frac{\mu-r}{2}}|u^{(m)}|_{r,w^{(\alpha+m,\beta+m)}},\end{aligned}$$

where $m-1<\nu\leqslant m$.

Proof. Using the properties of the Riemann–Liouville fractional integral operator leads to

$$D^{\nu}u(t)=I^{m-\nu}D^{m}u(t)=\frac{1}{\Gamma(m-\nu)}\int_0^t(t-s)^{m-\nu-1}D^{m}u(s)ds.$$

So, by means of Lemma 7 and then Lemma 6, respectively, one has

$$\begin{aligned}
&\|D^{\nu}u-D^{\nu}\mathcal{P}_{N,\alpha,\beta}u\|_{\mu,w^{(\alpha+m,\beta+m)}}\\
&=\|I^{m-\nu}(D^{m}u-D^{m}\mathcal{P}_{N,\alpha,\beta}u)\|_{\mu,w^{(\alpha+m,\beta+m)}}\\
&=\frac{1}{\Gamma(m-\nu)}\left\|\int_0^t(t-s)^{m-\nu-1}(D^{m}u(s)-D^{m}\mathcal{P}_{N,\alpha,\beta}u(s))\ ds\right\|_{\mu,w^{(\alpha+m,\beta+m)}}\\
&\leqslant\frac{\rho}{\Gamma(m-\nu)}\|D^{m}u-D^{m}\mathcal{P}_{N,\alpha,\beta}u\|_{\mu,w^{(\alpha+m,\beta+m)}}\\
&\leqslant\frac{\rho\ c'}{\Gamma(m-\nu)}\Big((N+m)(N+m+\alpha+\beta)\Big)^{\frac{\mu-r}{2}}|u^{(m)}|_{r,w^{(\alpha+m,\beta+m)}}.
\end{aligned}$$

□

Now, consider (16) again. If $y_N(t)$ is an approximate solution to $y(t)$, then the residual function is as follows:

$$H_N(t)=D^{\nu}y_N(t)+h(t)\ y_N(t)+\int_0^t k_N(t,s)\ y_N(s)\ ds+\int_0^t\widetilde{k}_N(t,s)\ D^{\gamma}y_N(s)\ ds-f(t). \tag{35}$$

The next lemma estimates a bound for residual function (35), which tends to zero when N tends to infinity.

Lemma 8. Let $r\in\mathbb{N}$, $\mu\in\mathbb{R}$, and $0\leqslant\mu\leqslant r$. Let us consider the residual function given in (35). When $N\to\infty$ one has $H_N(t)\to 0$.

Proof. Subtracting (35) from (16) and setting $e_N(t)=y(t)-y_N(t)$, as error function, leads to the following equation:

$$\begin{aligned}
H_N(t)=&-D^{\nu}(y(t)-y_N(t))-h(t)\ e_N(t)\\
&+\int_0^t k(t,s)\ y(s)\ ds-\int_0^t k_N(t,s)\ y_N(s)\ ds\\
&+\int_0^t\widetilde{k}(t,s)\ D^{\gamma}y(s)\ ds-\int_0^t\widetilde{k}_N(t,s)\ D^{\gamma}y_N(s)\ ds.
\end{aligned}\tag{36}$$

After some manipulation, (36) leads to the following equation:

$$\begin{aligned} H_N(t) = &-D^{\nu}(y(t)-y_N(t)) - h(t)\ e_N(t) \\ &+ \int_0^t k(t,s)\ e_N(s)\ ds + \int_0^t (k(t,s)-k_N(t,s))\ y_N(s)\ ds \\ &+ \int_0^t \tilde{k}(t,s) D^{\gamma}(y(s)-y_N(s))\ ds + \int_0^t (\tilde{k}(t,s)-\tilde{k}_N(t,s)) D^{\gamma} y_N(s)\ ds. \end{aligned} \tag{37}$$

Now, a bound is computed for residual function (37) so that

$$\|H_N\|_{\mu,w^{(\alpha,\beta)}} \leqslant G_1+G_2+G_3+G_4+G_5+G_6, \tag{38}$$

$$\|H_N\|_{\mu,w^{(\alpha,\beta)}} \leqslant G_1+G_2+G_3+G_4+G_5+G_6, \tag{39}$$

where

$$\begin{aligned} &G_1 = \|D^{\nu}(y-y_N)\|_{\mu,w^{(\alpha,\beta)}}, \qquad G_2 = \|h(t)\ e_N(t)\|_{\mu,w^{(\alpha,\beta)}}, \\ &G_3 = \left\| \int_0^t k(t,s)\ e_N(s)\ ds \right\|_{\mu,w^{(\alpha,\beta)}}, \\ &G_4 = \left\| \int_0^t (k(t,s)-k_N(t,s))\ y_N(s)\ ds \right\|_{\mu,w^{(\alpha,\beta)}}, \\ &G_5 = \left\| \int_0^t \tilde{k}(t,s) D^{\gamma}(y(s)-y_N(s))\ ds \right\|_{\mu,w^{(\alpha,\beta)}}, \\ &G_6 = \left\| \int_0^t (\tilde{k}(t,s)-\tilde{k}_N(t,s)) D^{\gamma} y_N(s)\ ds \right\|_{\mu,w^{(\alpha,\beta)}}. \end{aligned}$$

Using Theorem 6 leads to the following bound for G_1:

$$G_1 = \|D^{\nu}(y-y_N)\|_{\mu,w^{(\alpha,\beta)}} \leqslant \frac{c_0}{\Gamma(m-\nu)} \Big((N+m)(N+m+\alpha+\beta)\Big)^{\frac{\mu-r}{2}} |y^{(m)}|_{r,w^{(\alpha+m,\beta+m)}},$$

where $m=\lceil \nu \rceil$. According to continuity of function $h(t)$ over $[0,1]$, there exists $M_h>0$ such that $||h|| \leqslant M_h$. So, using Theorem 5 one has

$$G_2 = \|h(t)\ e_N(t)\|_{\mu,w^{(\alpha,\beta)}} \leqslant c_1\ M_h\ \Big(N(N+\alpha+\beta)\Big)^{\frac{\mu-r}{2}} |y|_{r,w^{(\alpha,\beta)}}.$$

By applying Lemma 7 and Theorem 5, a bound can be computed for G_3 as follows:

$$G_3 = \left\| \int_0^t k(t,s)\ e_N(s)\ ds \right\|_{\mu,w^{(\alpha,\beta)}} \leqslant \rho_1\ \|e_N(t)\|_{\mu,w^{(\alpha,\beta)}}$$

$$\leqslant \rho_1 \ c_1 \Big(N(N+\alpha+\beta) \Big)^{\frac{\mu-r}{2}} |y|_{r,w^{(\alpha,\beta)}}.$$

Now, define $e(k_N) = k(t,s) - k_N(t,s)$. Employing Lemma 7 and Corollary 1, respectively, provide the following bound for G_4:

$$G_4 = \left\| \int_0^t (k(t,s) - k_N(t,s)) \ y_N(s) \ ds \right\|_{\mu,w^{(\alpha,\beta)}} \leqslant \rho_2 \|e(k_N)\|_{\mu,w^{(\alpha,\beta)}}$$
$$\leqslant \rho_2 \ c_2 \ \Big(N(N+\alpha+\beta) \Big)^{\mu-r} |k(t,s)|_{r,W^{(\alpha,\beta)}}.$$

Again, based on Lemma 7 and Theorem 6, the following bound is obtained for G_5:

$$G_5 = \left\| \int_0^t \tilde{k}(t,s) D^{\gamma}(y(s) - y_N(s)) \ ds \right\|_{\mu,w^{(\alpha,\beta)}} \leqslant \rho_3 \ \left\| D^{\gamma} e_N(s) \right\|_{\mu,w^{(\alpha,\beta)}}$$
$$\leqslant \frac{\rho_3 \ c_3}{\Gamma(m_1-\gamma)} \ \Big((N+m_1)(N+m_1+\alpha+\beta) \Big)^{\frac{\mu-r}{2}} \ |y^{(m_1)}|_{r,w^{(\alpha+m_1,\beta+m_1)}},$$

where $m_1 = \lceil \gamma \rceil$. Defining $e(\tilde{k}_N) = \tilde{k}(t,s) - \tilde{k}_N(t,s)$ and using Lemma 7 and Corollary 1 lead to a bound for G_6 as follows:

$$G_6 = \left\| \int_0^t D^{\gamma} y_N(s)(\tilde{k}(t,s) - \tilde{k}_N(t,s)) \ ds \right\|_{\mu,w^{(\alpha,\beta)}} \leqslant \rho_4 \ \|e(\tilde{k}_N)\|_{\mu,w^{(\alpha,\beta)}}$$
$$\leqslant \rho_4 \ c_4 \ \Big(N(N+\alpha+\beta) \Big)^{\mu-r} |\tilde{k}(t,s)|_{r,W^{(\alpha,\beta)}}.$$

Therefore, using the above bounds, inequality (38) will be as follows:

$$\begin{aligned} \|H_N\|_{\mu,w^{(\alpha,\beta)}} \leqslant & \frac{c_0}{\Gamma(m-\nu)} \Big((N+m)(N+m+\alpha+\beta) \Big)^{\frac{\mu-r}{2}} \ |y^{(m)}|_{r,w^{(\alpha+m,\beta+m)}} \\ & + (M_h + \rho_1) \ c_1 \Big(N(N+\alpha+\beta) \Big)^{\frac{\mu-r}{2}} |y|_{r,w^{(\alpha,\beta)}} \\ & + (\rho_2 \ c_2 |k(t,s)|_{r,W^{(\alpha,\beta)}} + \rho_4 \ c_4 |\tilde{k}(t,s)|_{r,W^{(\alpha,\beta)}}) \Big(N(N+\alpha+\beta) \Big)^{\mu-r} \\ & + \frac{\rho_3 \ c_3}{\Gamma(m_1-\gamma)} \ \Big((N+m_1)(N+m_1+\alpha+\beta) \Big)^{\frac{\mu-r}{2}} \ |y^{(m_1)}|_{r,w^{(\alpha+m_1,\beta+m_1)}}. \end{aligned}$$

According to the continuity of the functions $y(t)$ and its derivatives, $k(t,s)$, and $\tilde{k}(t,s)$ over the compact intervals $[0,1]$ and $[0,1] \times [0,1]$, the residual function $H_N(t)$ becomes smaller as N is sufficiently large. Hence, the desired result is achieved. □

The following theorem presents an error bound for the proposed method.

Theorem 7. If $y_N(t)$ is the Jacobi approximate solution to $y(t)$, $e_N(t) = y(t) - y_N(t)$, $e(k_N) = k(t,s) - k_N(t,s)$, and $e(\tilde{k}_N) = \tilde{k}(t,s) - \tilde{k}_N(t,s)$ are the error functions, and $0 \leqslant \mu \leqslant r$, then $\|e_N\|_{\mu,w^{(\alpha,\beta)}} \to 0$ as $N \to \infty$.

Proof. It is clear that the function $y_N(t)$ is an approximate solution to problem (4), that is,

$$\begin{aligned} y_N(t) = F(t) + H_N(t) - \frac{1}{\Gamma(\nu)} \int_0^t (t-s)^{\nu-1} h(s)\; y_N(s)\; ds \\ - \frac{1}{\Gamma(\nu)} \int_0^t (t-s)^{\nu-1} \int_0^s k_N(s,s')\; y_N(s')\; ds'\; ds \\ - \frac{1}{\Gamma(\nu)} \int_0^t (t-s)^{\nu-1} \int_0^s \tilde{k}_N(s,s')\; D^\gamma y_N(s')\; ds'\; ds. \end{aligned} \tag{40}$$

So, by subtracting (39) from (4) and after some manipulations, the following error equation is obtained:

$$\begin{aligned} e_N(t) = -H_N(t) - \frac{1}{\Gamma(\nu)} \int_0^t (t-s)^{\nu-1} h(s)\; e_N(s)\; ds \\ - \frac{1}{\Gamma(\nu)} \int_0^t (t-s)^{\nu-1} \int_0^s k_N(s,s')\; e_N(s')\; ds'\; ds \\ - \frac{1}{\Gamma(\nu)} \int_0^t (t-s)^{\nu-1} \int_0^s y_N(s') e(k_N)\; ds'\; ds \\ - \frac{1}{\Gamma(\nu)} \int_0^t (t-s)^{\nu-1} \int_0^s \tilde{k}(s,s') D^\gamma e_N(s')\; ds'\; ds \\ - \frac{1}{\Gamma(\nu)} \int_0^t (t-s)^{\nu-1} \int_0^s D^\gamma y_N(s') e(\tilde{k}_N)\; ds'\; ds. \end{aligned} \tag{41}$$

A bound for (40) is calculated as follows:

$$\|e_N\|_{\mu,w^{(\alpha,\beta)}} \leqslant \|H_N\|_{\mu,w^{(\alpha,\beta)}} + Q_1 + Q_2 + Q_3 + Q_4 + Q_5, \tag{42}$$

where

$$\begin{aligned} Q_1 &= \frac{1}{\Gamma(\nu)} \left\| \int_0^t (t-s)^{\nu-1} h(s)\; e_N(s)\; ds \right\|_{\mu,w^{(\alpha,\beta)}}, \\ Q_2 &= \frac{1}{\Gamma(\nu)} \left\| \int_0^t (t-s)^{\nu-1} \int_0^s k_N(s,s')\; e_N(s')\; ds'\; ds \right\|_{\mu,w^{(\alpha,\beta)}}, \\ Q_3 &= \frac{1}{\Gamma(\nu)} \left\| \int_0^t (t-s)^{\nu-1} \int_0^s y_N(s') e(k_N)\; ds'\; ds \right\|_{\mu,w^{(\alpha,\beta)}}, \\ Q_4 &= \frac{1}{\Gamma(\nu)} \left\| \int_0^t (t-s)^{\nu-1} \int_0^s \tilde{k}(s,s') D^\gamma e_N(s')\; ds'\; ds \right\|_{\mu,w^{(\alpha,\beta)}}, \end{aligned}$$

$$Q_5 = \frac{1}{\Gamma(\nu)} \left\| \int_0^t (t-s)^{\nu-1} \int_0^s D^\gamma y_N(s') e(\tilde{k}_N)\ ds'\ ds \right\|_{\mu,w^{(\alpha,\beta)}}.$$

According to the continuity of the function $h(t)$, there exists M_h such that $||h|| \leqslant M_h$. Using Lemma 7 and Theorem 5, the following bounds are obtained for Q_1 and Q_2:

$$\begin{aligned} Q_1 &\leqslant \frac{1}{\Gamma(\nu)} \left\| \int_0^t (t-s)^{\nu-1} h(s)\ e_N(s)\ ds \right\|_{\mu,w^{(\alpha,\beta)}} \leqslant \frac{\rho_1}{\Gamma(\nu)} \| h(t)\ e_N(t) \|_{\mu,w^{(\alpha,\beta)}} \\ &\leqslant \frac{\rho_1\ M_h}{\Gamma(\nu)} \| e_N(t) \|_{\mu,w^{(\alpha,\beta)}} \leqslant \frac{\rho_1\ M_h\ c_0}{\Gamma(\nu)} \Big(N(N+\alpha+\beta) \Big)^{\frac{\mu-r}{2}} |y|_{r,w^{(\alpha,\beta)}}, \end{aligned}$$

$$\begin{aligned} Q_2 &\leqslant \frac{1}{\Gamma(\nu)} \left\| \int_0^t (t-s)^{\nu-1} \int_0^s k_N(s,s')\ e_N(s')\ ds'\ ds \right\|_{\mu,w^{(\alpha,\beta)}} \\ &\leqslant \frac{\rho_2}{\Gamma(\nu)} \left\| \int_0^s k_N(s,s')\ e_N(s')\ ds' \right\|_{\mu,w^{(\alpha,\beta)}} \leqslant \frac{\rho_2\ \rho_2'}{\Gamma(\nu)} \| e_N(t) \|_{\mu,w^{(\alpha,\beta)}} \\ &\leqslant \frac{\rho_2\ \rho_2'\ c_0}{\Gamma(\nu)} \Big(N(N+\alpha+\beta) \Big)^{\frac{\mu-r}{2}} |y|_{r,w^{(\alpha,\beta)}}. \end{aligned}$$

Applying Lemma 7 and Corollary 1 lead to the following bounds for Q_3 and Q_5:

$$\begin{aligned} Q_3 &= \frac{1}{\Gamma(\nu)} \left\| \int_0^t (t-s)^{\nu-1} \int_0^s y_N(s') e(k_N)\ ds'\ ds \right\|_{\mu,w^{(\alpha,\beta)}} \\ &\leqslant \frac{\rho_3}{\Gamma(\nu)} \left\| \int_0^s y_N(s') e(k_N)\ ds' \right\|_{\mu,w^{(\alpha,\beta)}} \leqslant \frac{\rho_3\ \rho_3'}{\Gamma(\nu)} \| e(k_N) \|_{\mu,w^{(\alpha,\beta)}} \\ &\leqslant \frac{\rho_3\ \rho_3'\ c_1}{\Gamma(\nu)} \Big(N(N+\alpha+\beta) \Big)^{\mu-r} |k(t,s)|_{r,W^{(\alpha,\beta)}}, \end{aligned}$$

$$\begin{aligned} Q_5 &= \frac{1}{\Gamma(\nu)} \left\| \int_0^t (t-s)^{\nu-1} \int_0^s D^\gamma y_N(s') e(\tilde{k}_N)\ ds'\ ds \right\|_{\mu,w^{(\alpha,\beta)}} \\ &\leqslant \frac{\rho_5}{\Gamma(\nu)} \left\| \int_0^s D^\gamma y_N(s') e(\tilde{k}_N)\ ds'\ ds' \right\|_{\mu,w^{(\alpha,\beta)}} \leqslant \frac{\rho_5\ \rho_5'}{\Gamma(\nu)} \| e(\tilde{k}_N) \|_{\mu,w^{(\alpha,\beta)}} \\ &\leqslant \frac{\rho_5\ \rho_5'\ c_3}{\Gamma(\nu)} \Big(N(N+\alpha+\beta) \Big)^{\mu-r} |\tilde{k}(t,s)|_{r,W^{(\alpha,\beta)}}. \end{aligned}$$

In order to compute a bound for Q_4, Lemma 7 and Theorem 6 are employed. So, one has

$$\begin{aligned}
Q_4 &= \frac{1}{\Gamma(\nu)}\left\| \int_0^t (t-s)^{\nu-1} \int_0^s \tilde{k}(s,s') D^{\gamma} e_N(s')\ ds'\ ds \right\|_{\mu,w^{(\alpha,\beta)}} \\
&\leqslant \frac{\rho_4}{\Gamma(\nu)}\left\| \int_0^s \tilde{k}(s,s') D^{\gamma} e_N(s')\ ds' \right\|_{\mu,w^{(\alpha,\beta)}} \leqslant \frac{\rho_4\ \rho_4'}{\Gamma(\nu)} \|D^{\gamma} e_N(t)\|_{\mu,w^{(\alpha,\beta)}} \\
&\leqslant \frac{\rho_4\ \rho_4'\ c_2}{\Gamma(m_1-\gamma)\ \Gamma(\nu)} \Big((N+m_1)(N+m_1+\alpha+\beta) \Big)^{\frac{\mu-r}{2}} |y^{(m_1)}|_{r,w^{(\alpha+m_1,\beta+m_1)}},
\end{aligned}$$

where $m_1 = \lceil \gamma \rceil$. Therefore, a bound will be computed for $\|e_N\|_{\mu,w^{(\alpha,\beta)}}$ as follows:

$$\begin{aligned}
\|e_N(t)\|_{\mu,w^{(\alpha,\beta)}} \leqslant \|H_N(t)\|_{\mu,w^{(\alpha,\beta)}} &+ \frac{1}{\Gamma(\nu)} \Big\{ (\rho_1\ M_h + \rho_2\ \rho_2')\ c_0 \Big(N(N+\alpha+\beta) \Big)^{\frac{\mu-r}{2}} |y|_{r,w^{(\alpha,\beta)}} \\
&+ (\rho_3\ \rho_3'\ c_1\ |k(t,s)|_{r,W^{(\alpha,\beta)}} + \rho_5\ \rho_5'\ c_3\ |\tilde{k}(t,s)|_{r,W^{(\alpha,\beta)}}) \Big(N(N+\alpha+\beta) \Big)^{\mu-r} \\
&+ \frac{\rho_4\ \rho_4'\ c_2}{\Gamma(m_1-\gamma)} \Big((N+m_1)(N+m_1+\alpha+\beta) \Big)^{\frac{\mu-r}{2}} |y^{(m_1)}|_{r,w^{(\alpha+m_1,\beta+m_1)}} \Big\}.
\end{aligned}$$

Hence, the desired result is acquired. □

Remark 4. The convergence of methods for (25) and (30) can be proved in a similar way. In order to approximate the nonlinear terms in (30), the following way is proposed:

$$y^2(t) - y_N^2(t) = (y(t) - y_N(t))(y(t) + y_N(t)) = e_N(t)(e_N(t) + 2y_N(t)).$$

Remark 5. In practice, to evaluate the effectiveness of the proposed method, the absolute errors of the approximate solutions obtained will be computed, provided that the exact solutions are available. For problems where exact solutions do not exist, the error equation, such as (40), will be solved using the same procedure suggested for the main problem, and an estimate of the absolute error will be obtained.

6 Numerical examples

In this section, the method presented in the previous section is applied to solve several examples taken from [16, 15, 53, 30, 28, 50] for comparison purposes. The proposed method is contrasted with the Homotopy Perturbation, Sinc-Collocation, Adomian Decomposition, Jacobi-Gauss integration, and Legendre and Bernoulli Wavelet methods, as discussed in [16, 15, 53, 30, 28, 50]. A comparison of the results is then provided. All computations were performed using Maple 13 software on a laptop equipped with an Intel R processor running at 2.20 GHz and 4.00 GB of RAM.

Example 1. As the first example, consider the following Volterra integro-differential equation of an arbitrary fractional order ν [53]:

$$D^{\nu} y(t) - t(1+2t) \int_0^t e^{s(t-s)}\ y(s)\ ds - 1 - 2t = 0, \qquad 0 \leqslant t \leqslant 1, \quad 0 < \nu \leqslant 1, \tag{43}$$

with initial condition $y(0) = 1$. If $\nu = 1$, then the exact solution is $y(t) = \exp(t^2)$. According to what expressed in section 4, the following approximations can be considered:

$$D^{\nu} y(t) \approx \Phi^T(t)\ C, \quad y(t) \approx \Phi^T(t)\ \mathbf{P}^{(\nu)\mathbf{T}}\ C + \Phi^T(t)\ F = \Phi^T(t)\ U,$$
$$e^{s(t-s)} \approx \Phi^T(t)\ K\ \Phi(s), \quad \int_0^t e^{s(t-s)}\ y(s)\ ds \approx \Phi(t)\ K\ \widetilde{U}\ \mathbf{P}\ \Phi(t),$$

where $y(0)$ is approximated as $\Phi^T(t)\ F$ and $\widetilde{U}$ is the operational matrix of product, corresponding to the vector $U = \mathbf{P}^{(\nu)\mathbf{T}}\ C + F$. Substituting the above approximations into (42) leads to the following algebraic equation:

$$\Phi^T(t)\ C - t(1+2t)\Phi(t)\ K\ \widetilde{U}\ \mathbf{P}\ \Phi(t) - 1 - 2t \approx 0. \tag{44}$$

By choosing $N = 10$, (43) is collocated at the roots of $P_{11}^{(\alpha,\beta)}(t)$. By arbitrarily selecting the values of the parameters α and β, the unknown vector C is determined by solving the resulting system. The maximum absolute errors for various values of α, β, $N = 10$, and $\nu = 1$ are listed in Table 1. Additionally, the estimated absolute errors, $Error_{Est}$, are computed and presented in Table 1. As shown, the estimated errors are in agreement with the absolute errors. (42) is solved in [53] using the Jacobi–Gauss integration method for $N = 2 : 2 : 20$ and $\nu = 1$. By choosing $N = 2 : 2 : 20$ and setting $\alpha = \beta = 0$, (43) is collocated at the roots of $P_{N+1}^{(0,0)}(t)$. By solving the resulting algebraic systems, the unknown vector C is determined, and the approximate solution can be obtained for any value of N. In Figure 1, the maximum absolute errors are plotted against N for $\alpha = \beta = 0$. It can be observed that the absolute errors decrease as N increases from 2 to 18, but for $N = 20$, the absolute error increases, which agrees with the results reported in [53]. The numerical results are shown in Figure 2 for values of $\nu = 0.25, 0.5, 0.75, 1$, $\alpha = 1/2$, $\beta = -1/2$, and $N = 10$. The approximate solutions for various values of ν and the exact solution are presented in part (a) of Figure 2. It can be observed that the numerical solutions converge to the analytic solution as ν approaches 1. Part (b) provides a graphical comparison between the exact and approximate solutions for $\nu = 1$.

Table 1: Maximum absolute and estimated errors for various values of α, β, $N = 10$, and $\nu = 1$ for Example 1

(α,β)	$Error_{Abs}$	$Error_{Est}$	(α,β)	$Error_{Abs}$	$Error_{Est}$
$(0,0)$	3.5146×10^{-8}	3.5187×10^{-8}	$(\frac{1}{2},\frac{1}{2})$	7.1293×10^{-8}	7.0560×10^{-8}
$(2,-\frac{1}{2})$	1.0013×10^{-6}	1.0012×10^{-6}	$(1,1)$	1.1774×10^{-7}	1.1786×10^{-7}
$(-\frac{1}{2},\frac{1}{2})$	1.5371×10^{-7}	1.5389×10^{-7}	$(\frac{1}{2},-\frac{1}{2})$	1.2362×10^{-7}	1.3083×10^{-7}
$(-\frac{1}{3},\frac{1}{4})$	8.1979×10^{-8}	8.2075×10^{-8}	$(-\frac{1}{4},-\frac{1}{5})$	2.5541×10^{-8}	2.5572×10^{-8}

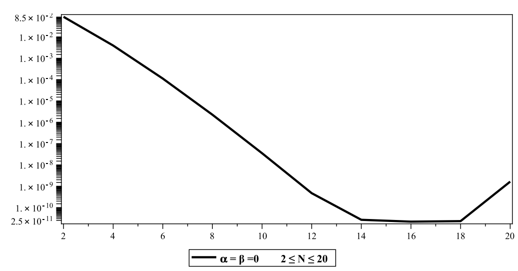

Figure 1: Maximum absolute error for different numbers of collocation points and $\alpha = \beta = 0$ for Example 1

Example 2. Consider the following linear FIDE [30]:

$$D^{\nu} y(t) - y(t) + \int_0^t y(s)\, ds - t(1+e^t) - 3e^t = 0, \qquad 0 \leqslant t \leqslant 1, \quad 3 < \nu \leqslant 4, \tag{45}$$

with initial conditions $y(0) = y'(0) = 1$, $y''(0) = 2$, and $y'''(0) = 3$. If $\nu = 4$ the exact solution is $y(t) = 1 + t\exp(t)$. Substituting the approximations given in the previous example into (44) leads to the following algebraic equation:

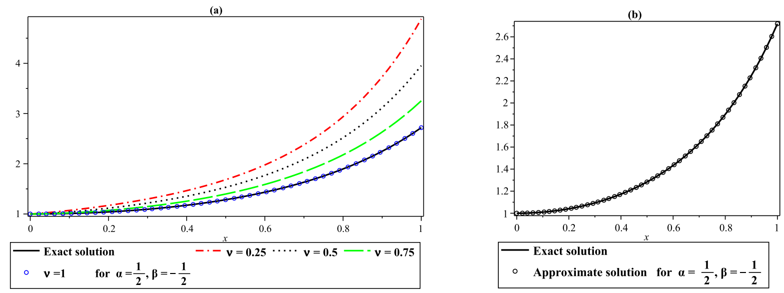

Figure 2: (a) Approximation solutions with different orders, ν, and exact solution, (b) Approximate and exact solutions for $\nu = 1$, $N = 10$, $\alpha = \frac{1}{2}$, and $\beta = -\frac{1}{2}$ for Example 1

$$\Phi^T(t)\ C - \left(\Phi^T(t)\ \mathbf{P}^{(\nu)\mathbf{T}}\ C + \Phi^T(t)\ F\right) + \Phi(t)\ K\ \widetilde{U}\ \mathbf{P}\ \Phi(t) - t(1+e^t) - 3e^t \approx 0, \tag{46}$$

where $1 + t + t^2 + t^3/2$ obtained from the initial conditions, is approximated as $\Phi^T(t)\ F$. By choosing $N = 10$ and setting $\nu = 4$ (the classical fourth-order integro-differential equation), (45) is collocated at the roots of $P_{11}^{(\alpha,\beta)}(t)$. By determining the values of the parameters α, β arbitrarily and solving the resultant algebraic system, the unknown vector C can be determined. Table 2 displays the maximum absolute errors for various values of α, β, and $N = 10$.

In Table 3, the values of the approximate and exact solutions are compared at the points $t_i = 0.2i, i = 0, 1, \ldots, 5$, for $\alpha = -1/4$, $\beta = -1/5$, and various values of ν. As shown in Table 3, the numerical values approach the exact values as $\nu \to 4$. A graphical comparison between the exact and approximate solutions is presented in Figure 3 for $\alpha = 1/3$, $\beta = 1/4$, and $N = 10$. It is evident from the figure that the numerical results converge to the exact solution as ν approaches 4.

Example 3. Consider the following nonlinear integro-differential equation with a fractional derivative of order ν [15]:

$$D^\nu y(t) + \int_0^t y^2(s)\ ds + \frac{t}{2} - \sinh(t) - \frac{1}{4}\sinh(2t) = 0, \qquad 0 \leqslant t \leqslant 1, \quad 0 < \nu \leqslant 2, \tag{47}$$

with initial conditions $y(0) = 0$ and $y'(0) = 1$. If $\nu = 2$ the exact solution is $y(t) = \sinh(t)$. By substituting the approximations given in Example 1 into (47), the following algebraic equation is obtained:

Table 2: Maximum absolute errors for various values of α, β, $N = 10$, and $\nu = 4$ for Example 2

(α, β)	$Error_{Abs}$	(α, β)	$Error_{Abs}$
$(0, 0)$	6.7806×10^{-13}	$(\frac{1}{2}, \frac{1}{2})$	1.3583×10^{-12}
$(-\frac{1}{5}, -\frac{1}{3})$	1.5960×10^{-12}	$(1, 1)$	2.2981×10^{-12}
$(-\frac{1}{2}, \frac{1}{2})$	2.6885×10^{-12}	$(\frac{1}{2}, -\frac{1}{2})$	2.5708×10^{-12}
$(\frac{1}{3}, \frac{1}{4})$	1.1678×10^{-12}	$(-\frac{1}{4}, -\frac{1}{5})$	4.8693×10^{-13}

Table 3: Approximate and exact solutions for different values of ν, $\alpha = -\frac{1}{4}$, $\beta = -\frac{1}{5}$, and $N = 10$ in Example 2

t_i	$\nu = 3.25$	$\nu = 3.50$	$\nu = 3.75$	$\nu = 3.90$	$\nu = 4$	Exact values
0.0	0.999999	0.999999	0.999999	0.999999	1.000000	1.000000
0.2	1.246742	1.245301	1.244608	1.244383	1.244280	1.244280
0.4	1.619754	1.607612	1.600653	1.598032	1.596729	1.596729
0.6	2.178540	2.136546	2.109904	2.098986	2.093271	2.093271
0.8	2.996977	2.895698	2.826706	2.796715	2.780432	2.780432
1.0	4.166138	3.965176	3.820669	3.754964	3.718281	3.718281

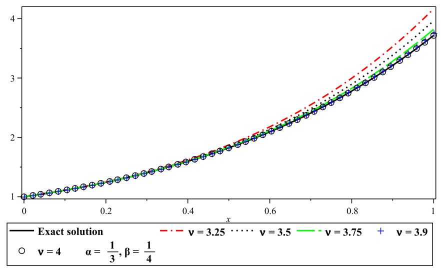

Figure 3: Approximation solutions with different values of ν and exact solution for $\alpha = \frac{1}{3}$, $\beta = \frac{1}{4}$, and $N = 10$ for Example 2

$$\Phi^T(t)\ C + \left(\Phi^T(t)\ \mathbf{P}^{(\nu)\mathbf{T}}\ C + \Phi^T(t)\ F\right) + \Phi(t)\ K\ \widetilde{U}\ \mathbf{P}\ \Phi(t) + \frac{t}{2} - \sinh(t) - \frac{1}{4}\sinh(2t) \approx 0, \tag{48}$$

where $\widetilde{U}$ is the operational matrix of the product corresponding to the vector $U = \mathbf{P}^{(\nu)\mathbf{T}}C + F$.

Table 4 displays the maximum absolute and estimated errors for various values of α, β, $\nu = 2$, and $N = 10$. The table shows that the numerical results are in good agreement with the exact solution. From Table 4, it can be observed that for cases where $\alpha = \beta$, the absolute errors decrease as the common values of α and β decrease. For $\alpha \neq \beta$, the absolute errors are smaller when $\alpha > \beta$. The estimated errors are also listed in Table 4. (47) is solved in [15] using the Homotopy Perturbation Method (HPM) and Variational Iteration Method (VIM) for $N = 2$. The results reported by [15] are depicted in part (a) of Figure 4. The plot of the approximate solution obtained by the Jacobi operational method is shown in part (b) of Figure 4 for $\alpha = \beta = 0$, $N = 2$, and $\nu = 2$. Based on Figure 4, it can be concluded that the result obtained by the Jacobi operational method is more precise than those obtained by VIM. In Table 5, the exact and approximate solutions are computed at the points $t_i = 0.2i, i = 0, 1, \ldots, 5$, for $\alpha = 1$, $\beta = -1/2$, and various values of ν. From Table 5, it can be seen that the numerical values approach the exact values as $\nu \to 2$. A graphical comparison between the exact and approximate solutions is presented in part (a) of Figure 5 for $\alpha = 1$, $\beta = -1/2$, and $N = 10$. Part (b) of Figure 5 plots the absolute error functions (i.e., the difference between the approximate results and the exact solution for $\nu = 2$). It can be observed that the absolute errors decrease as ν approaches 2.

Table 4: Maximum absolute and estimated errors for various values of α and β, $N = 10$, and $\nu = 2$ for Example 3

(α,β)	$Error_{Abs}$	$Error_{Est}$	(α,β)	$Error_{Abs}$	$Error_{Est}$
$(0,0)$	4.0258×10^{-14}	5.1161×10^{-12}	$(\frac{1}{2},\frac{1}{2})$	2.3641×10^{-13}	7.2078×10^{-12}
$(1,1)$	6.1463×10^{-13}	9.4707×10^{-12}	$(2,2)$	1.9956×10^{-12}	1.4367×10^{-11}
$(-\frac{1}{2},\frac{1}{2})$	3.5233×10^{-13}	1.3004×10^{-12}	$(\frac{1}{2},-\frac{1}{2})$	1.3970×10^{-13}	1.5617×10^{-12}
$(\frac{1}{3},\frac{1}{3})$	1.5246×10^{-13}	6.4781×10^{-12}	$(-\frac{1}{4},-\frac{1}{3})$	4.4786×10^{-14}	3.5623×10^{-12}
$(-\frac{1}{2},1)$	2.7671×10^{-12}	2.2636×10^{-11}	$(1,-\frac{1}{2})$	2.1062×10^{-13}	1.3716×10^{-12}

Table 5: Approximate and exact solutions for various values of ν, $\alpha = 1$, $\beta = -\frac{1}{2}$, and $N = 10$ in Example 3

t_i	$\nu = 1.25$	$\nu = 1.50$	$\nu = 1.75$	$\nu = 1.90$	$\nu = 2$	Exact values
0.0	1.8129×10^{-6}	8.7268×10^{-7}	2.1825×10^{-7}	5.1992×10^{-8}	4.6979×10^{-15}	0.000000
0.2	0.210520	0.205396	0.202710	0.201776	0.201336	0.201336
0.4	0.450364	0.430729	0.418353	0.413346	0.410752	0.410752
0.6	0.726395	0.685527	0.656555	0.643696	0.636653	0.636653
0.8	1.043130	0.977677	0.926485	0.902061	0.888105	0.888105
1.0	1.403192	1.314333	1.237566	1.198417	1.175201	1.175201

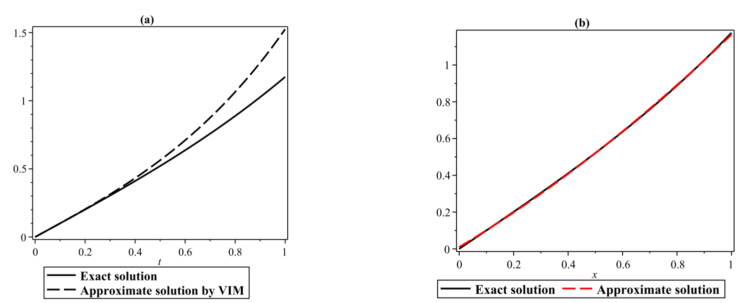

Figure 4: (a) Exact and approximate solutions obtained by VIM in Ref. [15], (b) Exact and approximate solutions obtained by Jacobi operational method for $\alpha = \beta = 0$, $N = 2$, and $\nu = 2$ for Example 3

Example 4. Consider the following mixed Volterra-Fredholm FIDE [28]:

$$D^{\nu+1}y(t)-\int_0^t (e^s+1)\, y^2(s)\, ds-\int_0^1 ts\, y^2(s)\, ds-g(t)=0, \qquad 0\leqslant t\leqslant 1,\ 0<\nu\leqslant 1, \quad (49)$$

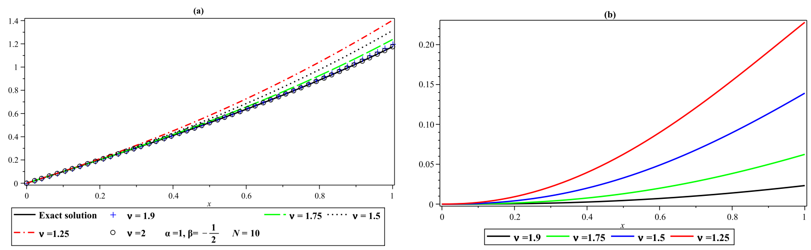

Figure 5: (a) Approximation solutions for different values of ν and exact solution, (b) Absolute error functions for $\alpha = 1$, $\beta = -\frac{1}{2}$, and $N = 10$ in Example 3

where $g(t) = \exp(t) - ((\exp(t) - t - 1)^3/3) - t(\exp(2)/4 - 2\exp(1) + 11/3)$. The initial conditions of problem are $y(0) = y'(0) = 0$ and its exact solution is $y(t) = \exp(t) - t - 1$ for $\nu = 1$. By applying the fundamental matrices, presented in section 4 for (49), the following algebraic equation is achieved:

$$\Phi^T(t)\ C - \Phi(t)\ K_1\ \widetilde{F}_2\ \mathbf{P}\ \Phi(t) - \Phi(t)\ K_2\ \mathbf{M}\ F_2 - g(t) \approx 0, \tag{50}$$

where $\widetilde{F}_2$ is the operational matrix of product, corresponding to the vector $F_2 = \widetilde{F}_1^T\ F_1$ where $F_1 = \mathbf{P}^{(\nu+1)\mathbf{T}}\ C$. Moreover, the matrix $\mathbf{M}$ is introduced in Remark 2. By choosing $N = 14$, (50) is collocated at the roots of $P_{15}^{(\alpha,\beta)}(t)$. By solving the resulting algebraic systems, the unknown vector C can be determined for $\alpha = \beta = 1$. In Table 6, the values of the exact and approximate solutions are compared at the points $t_i = 0.2i, i = 0, 1, \ldots, 5$, for various values of $\nu = 0.7, 0.8, 0.9, 0.99, 1$. It can be observed from Table 6 that the numerical values approach the exact values as ν approaches 1. Moreover, (49) is solved in [28] using the Legendre Wavelet method (LWM), and the numerical results are shown in part (a) of Figure 6. Additionally, a graphical comparison between the exact solution and the Jacobi approximate solution is provided in part (b) of Figure 6 for $\alpha = \beta = 1$, $N = 14$, and $\nu = 0.7, 0.8, 0.9, 0.99, 1$. Based on Figure 6, no significant difference is observed between the approximate solutions obtained using the Jacobi operational method and the LWM.

Example 5. Consider the following fractional-order integro-differential equation:

Table 6: Values of approximate and exact solutions at selected points for different values of ν, $\alpha=\beta=1$, and $N=14$ for Example 4

t_i	$\nu=0.7$	$\nu=0.8$	$\nu=0.9$	$\nu=0.99$	$\nu=1$	Exact values
0.0	-6.8186×10^{-5}	-2.3299×10^{-5}	-7.5562×10^{-6}	-4.9978×10^{-7}	7.1005×10^{-13}	0.000000
0.2	0.045519	0.035517	0.027619	0.021959	0.021403	0.021402
0.4	0.160712	0.133726	0.110976	0.093602	0.091834	0.091824
0.6	0.349039	0.300858	0.258855	0.225663	0.222222	0.222118
0.8	0.624058	0.550097	0.484580	0.431823	0.426292	0.425540
1.0	1.010148	0.902478	0.807252	0.730208	0.722096	0.718281

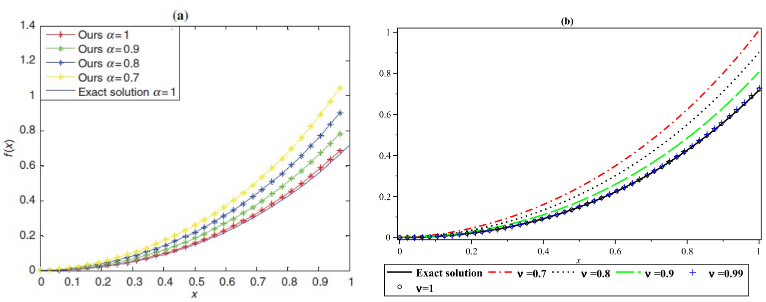

Figure 6: (a) Exact and approximate solutions obtained by LWM in Ref. [28], (b) Exact and approximate solutions obtained by Jacobi operational method for different values of ν, $\alpha=\beta=1$, and $N=14$ for Example 4

$$D^{\frac{1}{2}}y(t)+t^{\frac{3}{2}}\int_0^t (t+s)\,y(s)\,ds+\int_0^t ts\,D^{\frac{3}{8}}y(s)\,ds-g(t)=0, \qquad 0\leqslant t\leqslant 1, \quad (51)$$

where

$$g(t)=-\frac{2871928019}{3181474923}t^{\frac{5}{2}}+\frac{2850446155}{1841978638}t^{\frac{7}{2}}+\frac{3}{4}t^{\frac{11}{2}}-\frac{1}{2}t^{\frac{9}{2}}+\frac{11}{40}t^{6}-\frac{9}{40}x^{5}-\frac{1500440031}{8846634281}t^{\frac{45}{8}} + \frac{759388855}{3289964417}t^{\frac{53}{8}},$$

with initial condition $y(0)=0$ and exact solution $y(t)=3/4t^4-1/2t^3$.

By applying the fundamental matrices, presented in section 4 for (50), the following algebraic equation is resulted:

$$\Phi^T(t)\ C+t^{\frac{3}{2}}\Phi(t)\ K_1\ \widetilde{F}_1\ \mathbf{P}\ \Phi(t)+\Phi(t)\ K_2\ \widetilde{F}_2\ \mathbf{P}\ \Phi(t)-g(t)\approx 0, \qquad (52)$$

where the matrices $\widetilde{F}_1$ and $\widetilde{F}_2$ are the operational matrices of the product corresponding to the vectors $F_1=\mathbf{P}^{(\frac{1}{2})\mathbf{T}}C$ and $F_2=\mathbf{P}^{(\frac{1}{8})\mathbf{T}}C$, respectively. Table

7 presents the maximum absolute errors for various values of the parameters α and β with $N = 10$. The data in this table shows good agreement between the numerical results and the exact solution. In Table 8, the approximate solutions are calculated at equally spaced points $t_i = 0.1i, i = 0, 1, \ldots, 10$, for $N = 10$, $\alpha = -1/5$, $\beta = -1/4$, as well as for $\alpha = \beta = 2$. As observed, the error values change slowly over the interval $[0, 1]$, confirming the stability of the proposed method. A graphical comparison between the exact and approximate solutions, along with the plot of the absolute error function, is shown in parts (a) and (b) of Figure 7 for $\alpha = 1$, $\beta = 3$, and $N = 10$. Figure 7 demonstrates that the exact and approximate solutions are in good agreement. Additionally, the maximum absolute errors are plotted in Figure 8 for different numbers of collocation points, with $\alpha = 1/2$, $\beta = -1/2$, and various values of N (i.e., $N = 8 : 2 : 18$).

Table 7: Maximum absolute errors for various values of α and β and $N = 10$ for Example 5

(α, β)	$Error_{Abs}$	(α, β)	$Error_{Abs}$
$(0, 0)$	7.8229×10^{-7}	$(\frac{1}{2}, \frac{1}{2})$	1.5760×10^{-6}
$(1, 1)$	2.5249×10^{-6}	$(2, 2)$	4.6806×10^{-6}
$(-\frac{1}{2}, \frac{1}{2})$	1.9848×10^{-6}	$(\frac{1}{2}, -\frac{1}{2})$	1.9419×10^{-6}
$(-\frac{1}{2}, \frac{3}{4})$	1.8039×10^{-6}	$(1, \frac{1}{2})$	1.5760×10^{-6}
$(3, 1)$	7.0270×10^{-6}	$(1, 3)$	6.4222×10^{-6}
$(-\frac{1}{5}, -\frac{1}{4})$	3.9286×10^{-7}	$(\frac{1}{4}, \frac{1}{5})$	9.7123×10^{-4}

Example 6. Consider the following integro-differential equation with fractional derivative:

$$y''(t) + \frac{1}{t^2}\, y'(t) + \frac{1}{t}\, D^{0.7} y(t) = \int_0^t (6t^2 + 1)\, \cos(s)\, y(s)\, ds + g(t), \qquad 0 \leqslant t \leqslant 1, \tag{53}$$

where

$$\begin{aligned} g(t) = {} & (6t^6 - 71t^4 - 6t^7 + 132t^2 - 120t - 700t^3 + 24 + 119t^5) \sin(t) \\ & + (24t^5 - 140t^3 - 660t^2 + 355t^4 - 24t - 30t^6 - 120) \cos(t) \end{aligned}$$

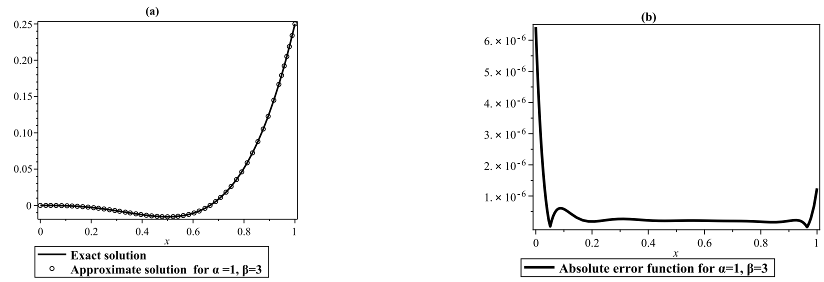

Figure 7: (a) Exact and approximate solutions, (b) Absolute error function for $\alpha = 1$, $\beta = 3$, and $N = 10$ for Example 5

Table 8: Values of absolute errors at some selected points for $N = 10$ of Example 5

t_i	Exact solution	$(\alpha, \beta) = (-\frac{1}{5}, -\frac{1}{4})$	$Error_{Abs}$	$(\alpha, \beta) = (2, 2)$	$Error_{Abs}$
0.0	0.000000000	-3.9286×10^{-7}	3.9286×10^{-7}	-4.6806×10^{-6}	4.6806×10^{-6}
0.1	-0.000425000	-0.000425109	1.0886×10^{-7}	-0.000425838	8.3841×10^{-7}
0.2	-0.002800000	-0.002799878	1.2197×10^{-7}	-0.002800614	6.1398×10^{-7}
0.3	-0.007425000	-0.007424974	2.6238×10^{-8}	-0.007425426	4.2625×10^{-7}
0.4	-0.012800000	-0.012800069	6.8770×10^{-8}	-0.012800338	3.3816×10^{-7}
0.5	-0.015625000	-0.015624900	1.0027×10^{-7}	-0.015625221	2.2117×10^{-7}
0.6	-0.010800000	-0.010800008	7.7315×10^{-9}	-0.010800155	1.5486×10^{-7}
0.7	0.008575000	0.008574946	5.4109×10^{-8}	0.008574919	8.0539×10^{-8}
0.8	0.051200000	0.051200089	8.8618×10^{-8}	0.051199977	2.2952×10^{-8}
0.9	0.127575000	0.127574902	9.7517×10^{-8}	0.127575027	2.6598×10^{-8}
1.0	0.250000000	0.249999746	2.5450×10^{-7}	0.249999155	8.4477×10^{-7}

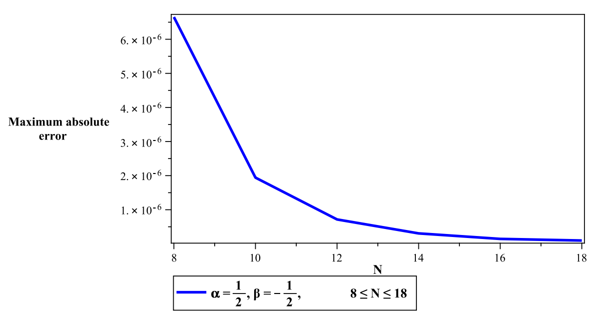

Figure 8: Maximum absolute error for different numbers of collocation points, $\alpha = \frac{1}{2}$, and $\beta = -\frac{1}{2}$ for Example 5

$$+ 20t^3 + 713t^2 - 4t + \frac{5995979123}{1902622932} t^{\frac{33}{10}} - \frac{6662541851}{2458295656} t^{\frac{23}{10}} + 120.$$

The initial conditions are $y(0) = y'(0) = 0$ and the exact solution does not exist. Following the process presented in case II in section 4 for (53) leads to the following algebraic equation:

$$\Phi^T(t)\, C + \frac{1}{t^2}\, \Phi(t)\, \mathbf{P}\, C + \frac{1}{t}\, \Phi(t)\, \mathbf{P^{(1.3)T}}\, C - \Phi(t)\, K\, \widetilde{F}\, \mathbf{P}\, \Phi(t) - g(t) \approx 0, \quad (54)$$

where the matrix $\widetilde{F}$ is the operational matrix of the product corresponding to the vector $F = (\mathbf{P^T})^{\mathbf{2}} C$. By choosing $N = 10$, (54) is collocated at the roots of $P_{11}^{(\alpha,\beta)}(t)$. By determining the values of the parameters α and β and solving the resulting algebraic system, the unknown vector C is determined. Since the exact solution of (53) is not available, the corresponding error equation is solved to estimate the absolute errors. Table 9 presents the maximum estimated errors for various values of the parameters α and β with $N = 10$. The maximum estimated errors are plotted in Figure 9 for different numbers of collocation points, where $\alpha = \beta = 0$ and various values of N (i.e., $N = 6 : 2 : 16$). In Table 10, the values of the approximate solutions are computed at the selected points $t_i = 0.2i, i = 1, 2, \ldots, 5$, for $N = 6, 10, 14$ and $\alpha = \beta = 0$. The maximum estimated errors decrease as N increases, and the values of the approximate solutions at the points t_i approach certain values with increasing N.

Table 9: Maximum estimated errors for various values of α and β and $N = 10$ for Example 6

(α, β)	$Error_{Est}$	(α, β)	$Error_{Est}$
$(0, 0)$	2.0157×10^{-9}	$(\frac{1}{2}, \frac{1}{2})$	2.3112×10^{-9}
$(1, 1)$	2.8243×10^{-9}	$(1, 2)$	1.9696×10^{-9}
$(-\frac{1}{2}, \frac{1}{2})$	2.0820×10^{-9}	$(\frac{1}{2}, -\frac{1}{2})$	1.1915×10^{-8}
$(-\frac{1}{3}, -\frac{1}{4})$	3.4068×10^{-9}	$(\frac{1}{4}, \frac{1}{5})$	1.5846×10^{-3}
$(\frac{1}{5}, -\frac{1}{3})$	1.7922×10^{-9}	$(2, 1)$	3.0742×10^{-8}

Example 7. Consider the following nonlinear integro-differential equation with fractional derivative of order ν [16]:

Table 10: Values of approximate solutions for $N = 6, 10, 14$, $\alpha = \beta = 0$ for Example 6

t_i	$N = 6$	$N = 10$	$N = 14$
0.2	-0.0012800925	-0.0012799986	-0.0012800001
0.4	-0.0153599943	-0.0153600011	-0.0153600000
0.6	-0.0518398699	-0.0518399999	-0.5184000000
0.8	-0.0819199727	-0.0819200001	-0.0819200000
1.0	6.3832×10^{-8}	1.4580×10^{-10}	3.4336×10^{-11}
$Error_{Est}$	1.5511×10^{-7}	2.0157×10^{-9}	1.8897×10^{-10}

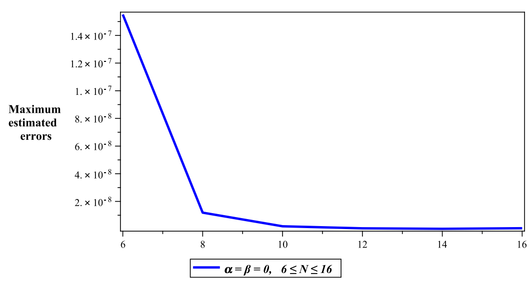

Figure 9: Maximum estimated error for various values of N and $\alpha = \beta = 0$ for Example 6

$$D^{\nu} y(t) = 1 + \int_0^t y(s)\ D^{\nu} y(s)\ ds, \qquad 0 \leqslant t \leqslant 1, \quad 0 < \nu \leqslant 1. \tag{55}$$

The initial condition for this example is $y(0) = 0$ and the exact solution is $y(t) = \sqrt{2}\tan(\sqrt{2}/2t)$ if $\nu = 1$. Following the process presented for nonlinear problems in section 4 for (55) leads to the following nonlinear algebraic equation:

$$\Phi^T(t)\ C - \Phi(t)\ K\ \widetilde{F}_2\ \mathbf{P}\ \Phi(t) - 1 \approx 0, \tag{56}$$

where the matrix $\widetilde{F}_2$ is the operational matrix of the product corresponding to the vector $F_2 = \widetilde{C}^T F_1$, where $F_1 = \mathbf{P}^{(\nu)\mathbf{T}} C$. Table 11 displays the maximum absolute errors for different values of α, β, and $N = 14$. The table demonstrates good consistency between the numerical results and the analytical solution. A graphical comparison between the exact and approximate solutions is shown in Figure 10 for values of $\nu = 0.5, 0.6, 0.7, 0.8, 0.9, 1$. (55)

has been solved using the Homotopy perturbation method (HPM), with the results reported in Ref. [16]. The absolute error functions of the approximate solutions can be seen in parts (a) (obtained by HPM) and (b) (obtained by the Jacobi operational method for $\alpha = 1/3, \beta = -1/4$) of Figure 11 for $N = 6$. It is evident that the error obtained by HPM is smaller than that obtained using the Jacobi operational method.

Table 11: Maximum absolute errors for various values of α and β, and $N = 14$ for Example 7

(α, β)	$Error_{Abs}$	(α, β)	$Error_{Abs}$
$(0, 0)$	3.2695×10^{-12}	$(\frac{1}{2}, \frac{1}{2})$	7.4506×10^{-12}
$(1, 1)$	1.3958×10^{-11}	$(2, 2)$	7.0196×10^{-11}
$(-\frac{1}{2}, \frac{1}{2})$	1.2529×10^{-12}	$(\frac{1}{2}, -\frac{1}{2})$	1.2842×10^{-11}
$(\frac{1}{3}, -\frac{1}{4})$	8.1919×10^{-12}	$(2, 1)$	5.5847×10^{-11}
$(-\frac{1}{3}, \frac{1}{4})$	1.0624×10^{-11}	$(1, 2)$	7.3824×10^{-11}

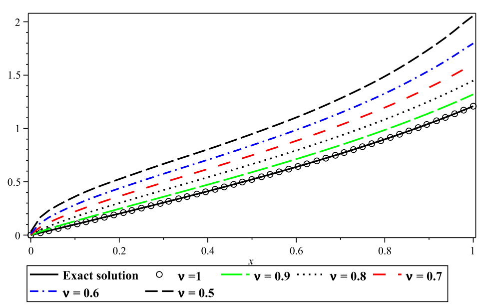

Figure 10: Approximate solutions for various values of ν, $N = 14$, $\alpha = \frac{1}{3}$, and $\beta = -\frac{1}{4}$ for Example 7

Example 8. Consider the following nonlinear system of integro-differential equations with fractional derivatives of order ν and γ [50]:

$$\begin{cases} D^{\nu}u(t) = u^2(t) + v^2(t) - \int_0^t u(s)\ ds, \\ D^{\gamma}v(t) = -\frac{1}{2}v^2(t) - u(t) - \int_0^t u(s)\ v(s)\ ds + \frac{1}{2}, \end{cases} \tag{57}$$

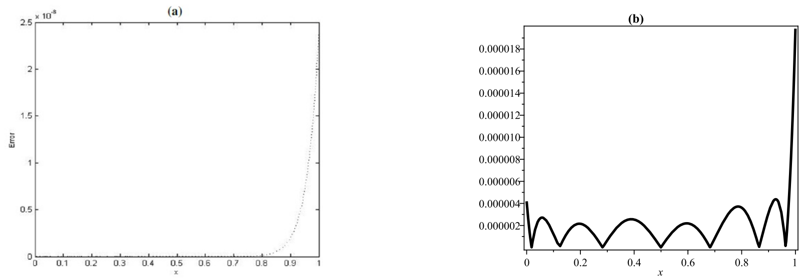

Figure 11: Absolute error function of approximate solution by :(a) HPM, (b) Jacobi operational method for $\alpha = \frac{1}{3}$, $\beta = -\frac{1}{4}$, and $N = 6$ in Example 7

where $0 < \nu, \gamma \leqslant 1$. The initial conditions for this example are $u(0) = 0$, $v(0) = 1$, and the exact solutions are $u(t) = \sin(t)$ and $v(t) = \cos(t)$ if $\nu = \gamma = 1$. Following the process presented for nonlinear problems in section 4 for system (57) leads to the following nonlinear system of algebraic equations:

$$\begin{cases} \Phi^T(t)\ C_1 - (\Phi^T(t)\ F_1)^2 - (\Phi^T(t)\ F_2)^2 + \Phi(t)\ K\ \widetilde{F}_1\ \mathbf{P}\ \Phi(t) \approx 0, \\ \Phi^T(t)\ C_2 + \frac{1}{2}(\Phi^T(t)\ F_2)^2 + \Phi^T(t)\ F_1 + \Phi(t)\ K\ \widetilde{U}\ \mathbf{P}\ \Phi(t) - \frac{1}{2} \approx 0, \end{cases} \tag{58}$$

where

$$\begin{aligned} &u(t) \approx \Phi^T(t)\ \mathbf{P}^{(\nu)T}\ C_1 = \Phi^T(t)\ F_1, \\ &v(t) \approx \Phi^T(t)\ \mathbf{P}^{(\gamma)T}\ C_2 + 1 \approx \Phi^T(t)\ \mathbf{P}^{(\gamma)T}\ C_2 + \Phi^T(t)\ V = \Phi^T(t)\ F_2, \\ &U = \widetilde{F}_2\ F_1. \end{aligned}$$

Table 12 displays the maximum absolute errors for different values of α, β, $\nu = \gamma = 1$, and $N = 10$. The table demonstrates good agreement between the numerical results and the analytical solutions. System (57) is solved using the Bernoulli wavelet method in [50]. The absolute errors of the approximate solutions, obtained by both the Jacobi collocation and Bernoulli wavelet methods, are calculated at the points $t_i = (2i-1)/16$, for $i = 1, 2, \ldots, 16$, and are shown in Tables 13 and 14. As seen, the results from the proposed method are more accurate (for $\alpha = -1/5$, $\beta = 1$, $\nu = \gamma = 1$, and $N = 10$). The approximate solutions obtained for $\nu = \gamma = 0.65, 0.75, 0.85, 0.95, 1$, $N = 10$, $\alpha = -1/3$, and $\beta = -1/4$ are depicted in Figure 12. It is evident that the approximate solutions approach the exact solutions as ν and γ approach 1.

Table 12: Maximum absolute errors of $u_{10}(t)$ and $v_{10}(t)$ for various values of α and β, and $\nu = \gamma = 1$ for Example 8

(α,β)	$Error_u$	$Error_v$	(α,β)	$Error_u$	$Error_v$
$(0,0)$	3.0826×10^{-14}	3.5991×10^{-14}	$(1,1)$	4.7157×10^{-13}	1.8738×10^{-13}
$(-\frac{1}{5},1)$	1.6600×10^{-12}	1.7294×10^{-12}	$(1,-\frac{1}{5})$	2.4327×10^{-13}	5.9886×10^{-13}
$(-\frac{1}{3},-\frac{1}{4})$	5.5345×10^{-14}	3.8509×10^{-14}	$(\frac{1}{2},-\frac{1}{2})$	1.0828×10^{-13}	1.3202×10^{-13}
$(-\frac{1}{2},\frac{1}{2})$	2.3938×10^{-13}	1.3725×10^{-13}	$(\frac{1}{2},\frac{1}{2})$	1.8085×10^{-13}	7.0934×10^{-14}

Table 13: Values of absolute errors of $u_{10}(t)$ at some points for $\alpha = -\frac{1}{5}, \beta = 1$ in Example 8

t_i	$Error_u$	$Error_u$ in [50]	t_i	$Error_u$	$Error_u$ in [50]
0.03125	8.7968×10^{-14}	4.51×10^{-5}	0.53125	8.1234×10^{-13}	6.87×10^{-4}
0.15625	2.3332×10^{-13}	2.20×10^{-4}	0.65625	1.0164×10^{-13}	8.24×10^{-4}
0.28125	4.2781×10^{-13}	3.68×10^{-4}	0.78125	1.2319×10^{-13}	9.55×10^{-4}
0.40625	6.1337×10^{-13}	5.41×10^{-4}	0.90625	1.4680×10^{-13}	1.08×10^{-3}

Table 14: Absolute errors of the approximate solution $v_{10}(t)$ for $\alpha = -\frac{1}{5}$ and $\beta = 1$ at selected points in Example 8

t_i	$Error_v$	$Error_v$ in [50]	t_i	$Error_v$	$Error_v$ in [50]
0.03125	7.8345×10^{-13}	4.77×10^{-4}	0.53125	5.8795×10^{-13}	1.05×10^{-4}
0.15625	7.3162×10^{-13}	4.19×10^{-4}	0.65625	4.7715×10^{-13}	4.59×10^{-5}
0.28125	6.7339×10^{-13}	3.38×10^{-4}	0.78125	3.5498×10^{-13}	2.18×10^{-4}
0.40625	6.3567×10^{-13}	2.33×10^{-4}	0.90625	2.1013×10^{-13}	4.11×10^{-4}

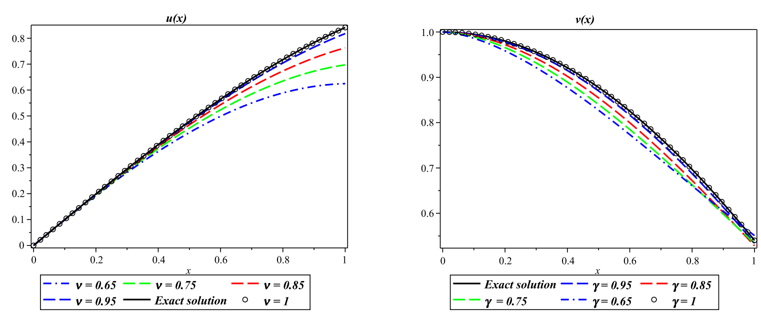

Figure 12: Appeoximate solutions for various values of ν and γ, $\alpha = -\frac{1}{3}, \beta = -\frac{1}{4}$, and $N = 10$ for Example 8

7 Conclusion

In this study, the Jacobi operational method has been successfully applied to solve both linear and nonlinear integro-differential equations involving fractional derivatives of arbitrary order ν. This method utilized shifted Jacobi polynomials defined on the interval $[0, 1]$, transforming the given problem, whether linear or nonlinear, into a set of more manageable algebraic equations. The resulting algebraic system is easier to solve compared to the original problem, highlighting a significant advantage of this approach. An additional strength of the proposed method is the straightforward determination of coefficients for the Jacobi series solution through the algorithms provided. Operational matrices for fractional integration and product are efficiently constructed using these algorithms. The study also investigated the existence and uniqueness of solutions for the equations and analyzed the convergence of the numerical approach. Illustrative examples provided in Examples 1–4, 7, and 8 showed that exact solutions exist only for integer values of ν. However, the numerical solutions obtained demonstrated strong agreement with the analytic solutions in these cases. For fractional values of ν within the range $m-1 < \nu < m$, where $m \in \mathbb{N}$, the numerical solutions gradually converge to the exact solutions as ν approaches m. In Example 5, where an exact solution is provided, the resulting absolute errors demonstrate the effectiveness of the proposed algorithm in solving such equations. Remarkably, Remark 5 offered a reliable method to estimate the absolute errors for the presented examples, which is particularly useful in scenarios like Example 6, where an exact solution is unavailable. The precision of the Jacobi operational method is further demonstrated by the consistently small and nearly uniform errors across the analyzed interval, affirming the validity of the Jacobi collocation method. A comparative analysis with other established methods, such as HPM, VIM, Sinc-collocation, Legendre wavelets, and Bernoulli wavelet methods, showed that the proposed technique produces more accurate results. Additionally, this method avoided the computational complexities of existing methods, such as Homotopy perturbation and Adomian decomposition, especially in determining Adomian polynomials. Based on the promising results obtained, it is expected that the Jacobi collocation method will become a robust tool for solving both linear and nonlinear functional equations. Future work aims to extend this method to address singular integro-differential equations with variable-order derivatives, although some modifications will be required. However, the method can be extended to higher-dimensional fractional equations, such as fractional integro-partial differential equations and partial differential equations with fractional orders. While the operational collocation method with Jacobi polynomials is effective for solving FIDEs in one dimension, applying it to higher dimensions presents challenges such as handling fractional derivatives in multiple dimensions, managing complex boundary conditions, ensuring numerical stability, and controlling computational costs. These challenges can be addressed by adopting a pseudo-operational approach.

CRediT authorship contribution statement

Khadijeh Sadri: Writing – review & editing, Writing-original draft, Visualization, Validation, Software, Resources, Methodology, Investigation, Formal analysis, Data curation, Conceptualization, Supervision. David Amilo: Writing-original draft, Validation, Formal analysis, Data curation. Evren Hincal: Visualization, Resources, Project administration.

Declaration of competing interest

The authors declare no conflicts of interest regarding the publication of this manuscript.

Data availability

Due to the nature of the research, supporting data is not available

Funding

This study receives no funding.

Acknowledgements

Authors are very grateful to anonymous referees for their careful reading and valuable comments which led to the improvement of this paper.

References

[1] Abbasbandy, S. *On convergence of homotopy analysis method and its application to fractional integro-differential equations*, Quaes. Math. 36 (2013), 93–105.

[2] Abdelkawy, M.A., Lopes, A.M. and Babatin, M.M. *Shifted fractional Jacobi collocation method for solving fractional functional differential equations of variable order*, Chaos. Soliton. Frac. 134 (2020), 109721.

[3] Abo-Gabal, H., Zaky, M.A. and Doha, E.H. *Fractional Romanovski–Jacobi tau method for time-fractional partial differential equations with nonsmooth solutions*, Appl. Num. Math. 182 (2022), 214–234.

[4] Ahmad, W.M. and El–Khazali, R. *Fractional-order dynamical models of love*, Chaos. Solit. Frac. 33 (2007), 1367–1375.

[5] Babaei, A., Jafari, H. and Banihashemi, S. *Numerical solution of variable order fractional nonlinear quadratic integro-differential equations based on the sixth-kind Chebyshev collocation method*, J. Comput. Appl. Math. 377 (2020), 112908.

[6] Bhrawy, A.H., Tharwat, M.M. and Yildirim, A. *A new formula for fractional integrals of Chebyshev polynomials: Application for solving multi-term fractional differential equations*, App. Math. Modelling. 37 (2013), 4245–4252.

[7] Biazar, J. and Sadri, K. *Solution of weakly singular fractional integro-differential equations by using a new operational approach*, J. Comput. Appl. Math. 352 (2019), 453–477.

[8] Chen, Y. and Tang, T. *Convergence analysis of the Jacobi spectral collocation methods for Volterra integral equations with a weakly singular kernel*, Math. Comput. 79 (2010), 147–167.

[9] Darweesh, A., Al-Khaled, K. and Al-Yaqeen, O.A. *Haar wavelets method for solving class of coupled systems of linear fractional Fredholm integro-differential equations*, Heliyon. 9(9) (2023), e19717.

[10] Dehestani, H., Ordokhani, Y. and Razzaghi, M. *Combination of Lucas wavelets with Legendre–Gauss quadrature for fractional Fredholm–Volterra integro-differential equations*, J. Comput. Appl. Math. 382 (2021), 113070.

[11] Dehghan, M. and Fakhar-Izadi, F. *The spectral collocation method with three different bases for solving a nonlinear partial differential equation arising in modeling of nonlinear waves*, Math. Comput. Model. 53 (2011), 1865–1877.

[12] Diethelm, A. and Free, D. *On the solution of nonlinear fractional-order differential equations used in the modeling of viscoplasticity, in: Scientific Computing in Chemical Engineering II: Computational Fluid Dynamics, Reaction Engineering, and Molecular Properties* (Eds. F. Keil, W. Mackens, H. Vob and J. Werther), Springer Verlag, Heidelberg, Pp. 217–224, 1999.

[13] Doha, E.H., Bhrawy, A.H. and Ezz-Eldien, S.S. *A new Jacobi operational matrix: An application for solving fractional differential equations*, App. Math. Modelling. 36 (2012), 4931–4943.

[14] Ebrahimi, H. and Sadri, K. *An operational approach for solving fractional pantograph differential equation*, Iranian J. Numer. Anal. Opt. 9(1) (2019), 37–68.

[15] Elbeleze, A.A., Kilicman, A. and Taib, B.M. *Approximate solution of integro-differential equation of fractional (arbitrary) order*, J. King Saud. Univ. Sci. 28(1) (2016), 61–68.

[16] Ghazanfari, B., Ghazanfari, A.G. and Veisi, F. *Homotopy Perturbation method for the nonlinear fractional integro-differential equations*, Aust. J. Basic. App. Sci. 4(12) (2010), 5823–5829.

[17] Guo, B.Y. and Wang, L.L. *Jacobi approximations in non-uniformly Jacobi-weighted Sobolev spaces*, J. Approx. Theory. 128 (2004), 1–41.

[18] He, J.H. *Nonlinear oscillation with fractional derivative and its applications*, In: International Conference on Vibrating Engineering, Dalian, China, pp. 288–291, 1998.

[19] He, J.H. *Some applications of nonlinear fractional differential equations and their approximations*. Bull. Sci. Technol. 15 (1999), 86–90.

[20] Heydari, M.H., Zhagharian, Sh. and Razzaghi, M. *Jacobi polynomials for the numerical solution of multi-dimensional stochastic multi-order time fractional diffusion-wave equations*, Comput. Math. Appl. 152 (2023), 91–101.

[21] Hosseininia, M., Heydari, M.H. and Avazzadeh, Z. *Orthonormal shifted discrete Legendre polynomials for the variable-order fractional extended Fisher–Kolmogorov equation*, Chaos. Soliton. Frac. 155 (2022), 111729.

[22] Huang, L., Li, X.F., Zhaoa, Y. and Duan, X.Y. *Approximate solution of fractional integro-differential equations by Taylor expansion method*, Comput. Math. App. 62 (2011), 1127–1134.

[23] Keskin, Y., Karaoglu, O., Servi, S. and Oturan, G. *The approximate solution of high order linear fractional differential equations with variable coefficients in term of generalized Taylor series*, Math. Comput. App. 16 (2011), 617–629.

[24] Khader, M.M. and Sweilam, N.H. *On the approximate solutions for system of fractional integro-differential equations using Chebyshev pseudo-spectral method*, Appl. Math. Modelling. 37(24) (2013), 9819–9828.

[25] Kumar, K., Pandey, R.K. and Sharma, S. *Comparative study of three numerical schemes for fractional integro-Differential equations*, J. Comput. App. Math. 315 (2017), 287–302.

[26] Li, X.J. and Xu, C.J. *A space-time spectral method for the time fractional diffusion equation*, SIAM. J. Numer. Anal. 47(3) (2009), 2108–2131.

[27] Mainardi, F. *Fractals and Fractional Calculus Continuum Mechanics*, Springer Verlag, Pp, 291–348, 1997.

[28] Meng, Z., Wang, L., Li, H. and Zhang, W. *Legendre wavelets method for solving fractional integro-differential equations*, Int. J. Comput. Math. 92(6) (2015), 1275–1291.

[29] Mokhtary, P. *Discrete Galerkin method for fractional integro-differential equations*, Acta. Math. Sci. 36B(2) (2016), 560–578.

[30] Momani, S. and Noor, M.A. *Numerical methods for fourth-order fractional integro-differential equations*, App. Math. Comput. 182 (2006), 754–760.

[31] Nazari Susahab, D., Shahmorad, S. and Jahanshahi, M. *Efficient quadrature rules for solving nonlinear fractional integro-differential equations of the Hammerstein type*, App. Math. Modelling. 39(18) (2015), 5452–5458.

[32] Rahimkhani, P. and Ordokhani, Y. *A numerical scheme based on Bernoulli wavelets and collocation method for solving fractional partial differential equations with Dirichlet boundary conditions.* Numer. Methods Partial Differ. Equ. 35(1) (2019), 34–59.

[33] Rahimkhani, P., Ordokhani, Y. and Babolian, E. *An efficient approximate method for solving delay fractional optimal control problems*, Nonlinear. Dyn. 86 (2016), 1649—1661.

[34] Rahimkhani, P., Ordokhani, Y. and Babolian, E. *A new operational matrix based on Bernoulli wavelets for solving fractional delay differential equations*, Numer. Algor. 74 (2017), 223—245.

[35] Rahimkhani, P., Ordokhani, Y. and Babolian, E. *Numerical solution of fractional pantograph differential equations by using generalized fractional-order Bernoulli wavelet*, J. Comput. Appl. Math. 309 (2017), 493–510.

[36] Rahimkhani, P., Ordokhani, Y. and Babolian, E. *Fractional-order Bernoulli functions and their applications in solving fractional Fredholem–Volterra integro-differential equations*. Appl. Numer. Math. 122 (2017), 66–81.

[37] Rahimkhani, P., Ordokhani, Y. and Babolian, E. *Muntz–Legendre wavelet operational matrix of fractional-order integration and its applications for solving the fractional pantograph differential equations*, Numer. Algor. 77 (2018), 1283—1305.

[38] Sadek, L. *A cotangent fractional derivative with the application*, Fractal Fract. 7(6) (2023), 444.

[39] Sadek, L., Baleanu, D., Abdo, M.S. and Shatanawi, W. *Introducing novel* Θ*-fractional operators: Advances in fractional calculus*, J. King Saud University - Sci. 36(9) (2024), 103352.

[40] Sadek, L. and Bataineh, A.S. *The general Bernstein function: Application to* χ*-fractional differential equations*, Math. Method. Appl. Sci. 47(7), (2024) 6117–6142.

[41] Sadek, L., Bataineh, A.S., Isik, O.R., Alaoui, H.T. and Hashim, I. *A numerical approach based on Bernstein collocation method: Application to differential Lyapunov and Sylvester matrix equations*, Math. Comput. Simul. 212 (2023), 475–488.

[42] Sadek, L. and Lazar, T.A. *On Hilfer cotangent fractional derivative and a particular class of fractional problems*, AIMS Mathematics. 8(12) (2023), 28334–28352.

[43] Sadek, L., Ounamane, S., Abouzaid, B. and Sadek, E.M. *The Galerkin Bell method to solve the fractional optimal control problems with inequality constraints*, J. Comput. Sci. 77 (2024), 102244.

[44] Sadek, L. and Algefary, A. *On quantum trigonometric fractional calculus*, Alex. Eng. J. 120 (2025), 371–377.

[45] Sadri, K., Amini, A. and Cheng, C. *Low cost numerical solution for three-dimensional linear and nonlinear integral equations via three-dimensional Jacobi polynomials*, J. Comput. App. Math. 319 (2017), 493–513.

[46] Sadri, K., Amini, A. and Cheng, C. *A new numerical method for delay and advanced integro-differential equations*, Numer. Algor. 77 (2018), 381–412.

[47] Szego, G. *Orthogonal polynomials*, American Mathematical Society, Providence, Rhode Island, 1939.

[48] Tavares, D., Almeida, R. and Torres, D.F.M. *Caputo derivatives of fractional variable order: Numerical approximations*, Commun. Nonlinear Sci. Numer. Simul. 35 (2016), 69–87.

[49] Varol Bayram, D. and Daşcıoğlu, A. *A method for fractional Volterra integro-differential equations by Laguerre polynomials*, Adv. Differ. Equ. 2018 (2018), 466.

[50] Wang, J., Xu, T.Z., Wei, Y.Q. and Xie, J.Q. *Numerical simulation for coupled systems of nonlinear fractional order integro-differential equations via wavelets method*, Appl. Math. Comput. 324 (2018), 36–50.

[51] Yaghoubi, S., Aminikhah, H. and Sadri, K. *A new efficient method for solving yystem of weakly singular fractional integro-differential equations by shifted sixth-kind Chebyshev polynomials*, J. Math. 2022 (2022), 9087359.

[52] Yaghoubi, S., Aminikhah, H. and Sadri, K. *A spectral shifted Gegenbauer collocation method for fractional pantograph partial differential equations and its error analysis*, Sadhana. 48 (2023), 213.

[53] Yang, Y. *Convergence Analysis of the Jacobi Spectral-Collocation Method for Fractional Integro-Differential Equations*, Acta Math. Sci. 34(3) (2014), 673–690.